

Article

Uncovering the Fungal Diversity Colonizing Limestone Walls of a Forgotten Monument in the Central Region of Portugal by High-Throughput Sequencing and Culture-Based Methods

Diana S. Paiva ^{1,*}, Luís Fernandes ¹, João Trovão ^{1,2} , Nuno Mesquita ¹, Igor Tiago ¹  and António Portugal ^{1,2} 

¹ Centre for Functional Ecology (CFE)—Science for People & the Planet, Department of Life Sciences, University of Coimbra, Calçada Martim de Freitas, 3000-456 Coimbra, Portugal

² FitoLab—Laboratory for Phytopathology, Instituto Pedro Nunes, Rua Pedro Nunes, 3030-199 Coimbra, Portugal

* Correspondence: dpaivaphd@gmail.com

Featured Application: This work expands the current knowledge of fungal agents and their role in the biodeterioration of limestone rocks, while providing tools for the development of better and more adequate strategies for the conservation, restoration, and rehabilitation of the heritage. Although the information presented here is related to a single monument in Portugal, the data can be extrapolated to other monuments of similar lithology.

Abstract: Fungal organisms are considered one of the most relevant stone colonizers, and biodeteriogens. They are ubiquitous heterotrophs, metabolically versatile, ranging from generalist to extremophiles. Limestone, a sedimentary rock characterized by high levels of calcium carbonate, has low compressive strength and hardness and high porosity. These features make it highly susceptible to fungal colonization and an exceptional target for biodeterioration. Understanding the mycobiome composition associated with different biodeterioration scenarios is key for the development of effective guidelines and strategies for preventive conservation and viable maintenance of our cultural heritage. In this work, a thorough analysis of the fungal community composition on the Lemos Pantheon, a limestone-built artwork located in Portugal, was performed using high-throughput sequencing complemented with culture-based methods. The combined results allowed a detailed characterization of the fungal communities of each analyzed spot, revealing highly diverse and dissimilar communities according to the type of biodeterioration observed. In addition, we verified that both cultivation and metagenomics methodologies should be employed synergistically to tackle inherent limitations.

Keywords: biodeterioration; culture-dependent methodologies; cultural heritage; fungi; indoor; Ançã limestone; next-generation sequencing



Citation: Paiva, D.S.; Fernandes, L.; Trovão, J.; Mesquita, N.; Tiago, I.; Portugal, A. Uncovering the Fungal Diversity Colonizing Limestone Walls of a Forgotten Monument in the Central Region of Portugal by High-Throughput Sequencing and Culture-Based Methods. *Appl. Sci.* **2022**, *12*, 10650. <https://doi.org/10.3390/app122010650>

Academic Editor: Dimitris Mossialos

Received: 22 September 2022

Accepted: 17 October 2022

Published: 21 October 2022

Publisher's Note: MDPI stays neutral with regard to jurisdictional claims in published maps and institutional affiliations.



Copyright: © 2022 by the authors. Licensee MDPI, Basel, Switzerland. This article is an open access article distributed under the terms and conditions of the Creative Commons Attribution (CC BY) license (<https://creativecommons.org/licenses/by/4.0/>).

1. Introduction

The use of stone as a building material in monuments and artworks is an ancient practice and much of our built heritage is based on this type of material, given its abundance, mechanical and decorative properties and, especially, its durability. Limestone, a sedimentary rock characterized by high levels of calcium carbonate (CaCO₃), due to its properties and abundance in Portugal, particularly on the central coast, has been widely used in construction, both as a structural and as a decorative material [1].

The weathering of rocks, a fundamental step in the cycles of minerals on our planet, can become an inconvenient process with serious consequences when it affects stone used in construction [1,2]. This is a more pressing and relevant fact in buildings with historical and cultural value, resulting in immeasurable losses [3].

For several decades, the role of microorganisms in the deterioration of the cultural heritage was neglected, with emphasis being placed mainly on the effect of environmental and chemical factors. Recently, numerous studies have been carried out focusing on the relationship between microorganisms and stone monuments, revealing their relevance in the processes of deterioration of materials used in assets with historical and cultural value [4–18]. Nevertheless, it is impossible to separate the biological action from the physicochemical factors [19]. These agents act together, and in close relation, in an antagonistic or synergistic way, in the deterioration of the stone [1,2]. In this combined process, their relative importance varies with factors such as environmental conditions, the type of substrate, the state of conservation and location in the monument [20].

Colonization by microorganisms and subsequent biodeterioration, especially in the outdoors, cannot be controlled and is markedly influenced by climate and location [21]. However, in indoor environments, it is mainly influenced by human occupation and associated activities and can (to a certain extent) be controlled, particularly by managing lighting, heating, humidity, and ventilation [21,22]. The existence of water on the stone surface is considered one of the most determining factors in the occurrence of these phenomena [21,23].

Fungi are considered one of the most important stone colonizers [24]. They are ubiquitous heterotrophic organisms, metabolically more versatile than other biodeteriogenic agents, a characteristic that allows them to colonize a wide range of substrates, such as wood, metal, and stone, among others. The ability to grow on different substrates, resist extreme environmental conditions and adopt different structural, morphological, and metabolic strategies, makes them highly adaptable organisms capable of thriving in inhospitable environments [25]. They are particularly active in the biodeterioration of rock through several physical and chemical mechanisms, often with synergistic action, that can result in pitting, mineral dislocation, dissolution and reprecipitation [3,6,21,24,26,27]. Additionally, besides the ability to deeply alter stone integrity and structure, some fungi produce pigments (e.g., melanin) that cause chromatic alteration of the rock, an effect considered unaesthetic [6,26–29].

Limestones are carbonate rocks with a high intrinsic bioreceptivity, being especially prone to microbial colonization and, consequently, to biodeterioration phenomena. Ançã limestone, a subtype of limestone often used in Portuguese monuments, has the highest primary bioreceptivity among different Portuguese lithotypes [17]. Very few studies have been conducted targeting fungal colonization in this particular subtype of limestone, but Trovão et al. [16] revealed highly diverse fungal communities in this lithotype, that play an active role in the biodeterioration processes.

Until recently, most information available on the colonization of cultural property by microorganisms came from the use of classical microbiology methodologies. The exclusive use of culture-dependent methods is not enough to fully characterize microbial communities, detecting only a small fraction of the total diversity existing in a sample. This is verified not only because the growth conditions of many species are unknown, or difficult to reproduce, but also because of the existence of microorganisms in inactive (viable, but not cultivable) states [30–33]. To bypass this limitation, culture-independent methodologies, namely molecular biology techniques, have been extensively used in the profiling of microbiological communities in biodeterioration studies. These techniques, based on DNA analysis, allow the profiling of complex communities. Due to their implementation, some studies have shown that the microbiological diversity in this type of substrate is much greater than was previously believed [30–34]. High-throughput next-generation sequencing (HTS) has revolutionized the study of genomics and molecular biology by allowing, in a much faster way, the sequencing and analysis of billions of DNA fragments, providing a much more detailed representation of the populations present in a sample [35,36]. Nevertheless, only a small number of studies have been performed in which high-throughput sequencing was applied to limestone fungal populations in biodeterioration scenarios, particularly in Portugal [14,16,37].

Nonetheless, with advantages and disadvantages associated with both approaches, the classic microbiological methods complement molecular techniques in the identification, characterization, and description of microorganisms, allowing a better understanding of the real biodiversity within stone-colonizing communities [38].

The biological deterioration of the historical heritage is one of the greatest concerns of conservationists and restorers worldwide. Knowing and understanding the factors that lead to the alteration of rocks is, without a doubt, the first and most important step in the development of more appropriate and effective guidelines and strategies, in order that preventive conservation and viable maintenance of our cultural heritage can be carried out. However, given the numerous intrinsic and extrinsic factors associated with stone alteration, a definitive and universal solution is unlikely to be found.

Located in the central region of Portugal, the Church of Trofa houses the only element of the municipality of Agueda classified as a National Monument, officially integrated in the Portuguese Cultural Heritage. This classification arises from the fact that inside it has an emblematic sculptural-funerary ensemble of great architectural and artistic value—the Lemos Pantheon [39], that is barely known and rarely visited by tourists. After several years bearing a forgotten and degraded appearance, with biological colonization markedly affecting the limestone of this site, in August this year, restoration and requalification interventions were started, which included the cleaning of the interior and exterior façades [40], without a previous analysis or extensive knowledge of the biodeterioration phenomena present there. This posed a risk to the conservation of this monument that could lead to a future recolonization with potentially worse effects [41,42].

The objective of this work was to thoroughly characterize the fungal diversity associated with different biodeterioration phenomena present in this monument, using high-throughput next-generation sequencing and cultivation-dependent methodologies. This information will ultimately contribute to science-supported restoration plans in future interventions.

2. Materials and Methods

2.1. Location and Sampling

The Church of Trofa or Church of São Salvador da Trofa (Figure 1a) is a Catholic temple located in Trofa (Trofa do Vouga), in the Portuguese district of Aveiro, Águeda county (N 40 36.653' W 008 28.729'). This church houses the Lemos Pantheon (Figure 1b,c), a remarkable Renaissance sculptural ensemble dating from the 16th century, carved in white Ançã limestone, and attributed to the artist João de Ruão. Commissioned by D. Duarte de Lemos in 1534, the Lemos Pantheon presents itself as a burial place for the ancestors of the third lord of Trofa. It integrates two tombstone groups facing each other, both formed by two arches separated by pilasters and topped by an entablature. On the right-hand side are the tombs of the first lords of Trofa, Gomes Martins de Lemos and his son, João Gomes de Lemos, and their respective wives, D. Maria de Azevedo and D. Violante de Sequeira, leaving the men in the arch nearest the altar. On the opposite side lies buried D. Joana de Melo, wife of the founder, and in the arch closest to the altar D. Duarte de Lemos, with a praying statue [43].

The Church of Trofa, comprising the tombs of the Lemos family, has been classified as a National Monument since 1992 (IPA.00001042, decree of 16-06-1910, DG, nr 136, of 23-06-1910). More details about the monument, including photographs, can be accessed on the SIPA website [43], an online information and documentation system on the Portuguese architectural, urban and landscape heritage managed by the General Directorate for Cultural Heritage (DGPC). Despite being the most important local landmark, it is mainly used for local religious events. In general, the tomb complex is in a reasonable state of conservation; however, some areas present visible pathologies, severely affecting the limestone of this site both structurally and aesthetically.

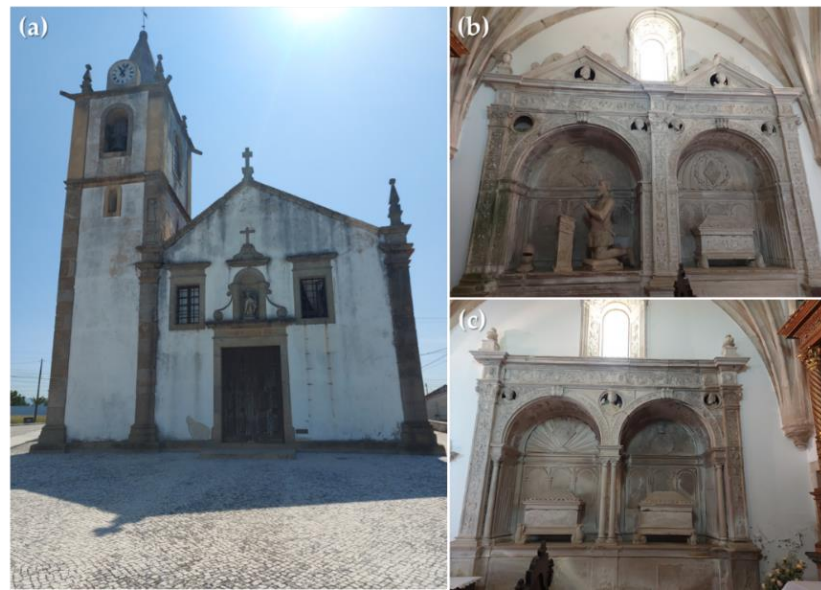


Figure 1. Study site (a) Church of Trofa do Vouga which houses the Lemos Pantheon. (b) Left side of the Pantheon comprising the tombs of D. Joana de Melo (on the right) and her husband, D. Duarte de Lemos (on the left), where the praying statue stands (c) Right side of the Pantheon comprising the tombs of Gomes Martins de Lemos and his son, João Gomes de Lemos (on the right), and their wives, D. Maria de Azevedo and D. Violante de Sequeira, respectively (on the left).

All samples were collected indoors in July 2021, during the summer season. A digital thermohygrometer was used to measure the temperature (T) and relative humidity (RH) inside, at the beginning and the end of the sampling procedure. The average values were T 22 °C and RH 51%. After careful observation, sampling was carried out on representative areas showing clear evidence of alteration and degradation. Four samples were collected from these areas (Figure 2) and distinct biodeterioration outlines found in these sites were classified based in the ICOMOS Illustrated glossary on stone deterioration patterns: L1—dark and green biofilm (DGB), L2—green biofilm (GB), L3—black discoloration (BD) and L4—salt efflorescence (SE) [44]. Microinvasive sampling using sterile scalpels by scrapping small areas (approximately 0.5 g) into a sterile petri dish, as well as noninvasive sampling by swabbing surfaces with sterile nitrocellulose discs (Ø 5 cm, 2 per sampling area) were carried out.



Figure 2. Details of the sampling points (a) L1, DGB at the base of the left pillar in D. Duarte de Lemos tomb; (b) L2, GB at the base of the right pillar in Gomes Martins de Lemos and his son, João Gomes de Lemos tomb; (c) L3, BD behind the tomb chest of D. Maria de Azevedo and D. Violante de Sequeira and (d) L4, SE beneath L3, closest to the floor.

Each collected sample (L1 to L4) was divided into two aliquots (each with ≈ 0.25 g and 1 disc): one for Illumina high-throughput sequencing, stored at -80 °C until further processing; and the other for direct fungal isolation, stored in the dark, at room temperature and processed within 4 h of collection.

2.2. Fungal High-Throughput Illumina Sequencing and Analysis

The total DNA of each aliquot (L1, L2, L3 and L4) was extracted using a Powersoil DNA Isolation Kit (Qiagen, Hilden, Germany), according to the manufacturer's instructions with minor modifications. Samples were prepared for Illumina Sequencing by Internal Transcribed Spacer 2 region amplification of the microbial community. The DNA was amplified for the hypervariable region with specific primers and further reamplified in a limited-cycle PCR reaction to add sequencing adapters and dual indexes. First PCR reactions were performed for each sample using a KAPA HiFi HotStart PCR Kit (Kapa Biosystems, Roche, Basel, Switzerland) according to the manufacturer's suggestions: 0.3 μ M of each PCR primer of a pool of forward primers ITS3NGS1_F 5'-CATCGATGAAGAACGCAG-3', ITS3NGS2_F 5'-CAACGATGAAGAACGCAG-3', ITS3NGS3_F 5'-CACCGATGAAGAACGCAG-3', ITS3NGS4_F 5'-CATCGATGAAGAACGTAG-3', ITS3NGS5_F 5'-CATCGATGAAGAACGTGG-3', and ITS3NGS10_F 5'-CATCGATGAAGAACGCTG-3' and reverse primer ITS4NGS001_R 5'-TCCTSCGCTTATTGATATGC-3' [45] and 5 μ L of template DNA in a total volume of 25 μ L. The PCR conditions involved a 3 min denaturation at 95 °C, followed by 35 cycles of 98 °C for 20 s, 60 °C for 30 s and 72 °C for 30 s and a final extension at 72 °C for 5 min. Second PCR reactions added indexes and sequencing adapters to both ends of the amplified target region according to the manufacturer's recommendations [46]. Negative PCR controls were included for all amplification procedures. PCR products were then one-step purified and normalized using a SequalPrep 96-well plate kit (ThermoFisher Scientific, Waltham, MA, USA) [47], pooled and pair-end sequenced in the Illumina MiSeq[®] sequencer with the MiSeq Reagent Kit v3 (600 cycles), according to the manufacturer's instructions (Illumina, San Diego, CA, USA) at GenoInseq, Next Generation Sequencing Unit of CNC/Biocant (Cantanhede, Portugal).

Treatment of metabarcoding raw data, clustering and taxonomic analyses were performed at GenoInseq, Next Generation Sequencing Unit of CNC/Biocant (Cantanhede, Portugal). Raw reads were extracted from an Illumina MiSeq[®] System in fastq format and quality filtered with a PRINSEQ version 0.20.4 [48] to remove sequencing adapters, trim bases with an average quality lower than Q25 in a window of five bases and eliminate reads with fewer than 100 bases. The forward and reverse reads were merged by overlapping paired end reads with an AdapterRemoval version 2.1.5 [49] using default parameters. The QIIME2 package version 2020.2 [50] was used for operational taxonomic unit (OTU) generation, taxonomic identification, sample diversity and richness indices calculation. Sample IDs were assigned to the merged reads and converted to FASTA format. Chimeric merged reads were detected and removed using UCHIME [51] against the UNITE/QIIME ITS database version 8.2 [52]. The ITSx version 1.1.2 [53] was used to extract the highly variable fungal ITS2 subregion from the merged reads. OTUs were selected at 97% similarity threshold using the open reference strategy and those with fewer than two reads were removed from the OTU table. A representative sequence of each OTU was then selected for taxonomy assignment using the referred database. All metagenomic data were deposited in the international SRA database with the reference PRJNA875387.

2.3. Statistical Analysis

Alpha diversity indices Chao1, Abundance-based Coverage, Dominance, Equitability, Goods Coverage, observed OTUs, Shannon and Simpson were calculated using a PAST software package (v.4.09 <https://www.nhm.uio.no/english/research/resources/past/> (accessed on 3 June 2022)) to reflect the diversity and richness of the fungal communities in the different samples (L1, L2, L3 and L4).

The community structure was analyzed based on the relative abundance at different classification levels. The relative abundance of individual taxa within each sample was estimated by comparing the number of sequences assigned to a specific taxon with the number of total sequences obtained for that sample. For this purpose, Microsoft® Excel® 2016 software was used to process the raw OTU table, and to analyze and visualize the results. Due to the high number of taxa present in each sample, only the 20 most abundant were detailed in the graphs.

Beta diversity analysis was performed using principal coordinate analysis (PCoA) ordination, based on the Bray–Curtis’s dissimilarity matrix, generated from the relative abundance of fungal genera, and the unweighted pair-group method with arithmetic means (UPGMA) clustering were both performed using a PAST software package v.4.09. Using the same software, differences between the community structures within a site were tested by permutational multivariate analysis of variance (PERMANOVA) and further analyzed through a SIMPER test.

Between samples, a Venn analysis was constructed to identify unique and common fungal genera using an InteractiVenn online tool [54]. Prevalence within each sample for the 20 most abundant genera was evaluated in a Clustvis web tool through a Heatmap [55].

2.4. Culturable Fungal Isolation, Identification and Analysis

For direct fungal isolation each aliquot was suspended in 2 mL of sterile 0.9% (*w/v*) NaCl solution, and vortexed. A volume of 100 µL was inoculated in six different culture media: potato dextrose agar (PDA); dichloran-glycerol agar (DG-18); malt extract agar supplemented with 10% NaCl (*w/v*) (MEA 10%); Czapek solution agar (CZ); rose bengal agar base (RB) and DSMZ 372-Halobacteria medium supplemented with 10% NaCl (*w/v*) (HM 10%), in triplicate. All culture media were supplemented with streptomycin (0.5 gL⁻¹) to prevent bacterial growth. Inoculated media plates were incubated aerobically, in the dark, at 25 ± 2 °C, for 6 months. Emerging colonies showing significantly different morphologies (in each culture medium) were isolated to axenic cultures for DNA extraction. DNA extraction from pure cultures was conducted with the REDextract-N.Amp™ Plant PCR Kit (Sigma Aldrich, St. Louis, MO, USA), with several modifications. A small portion (~1 mm²) of the colonies was scraped from the agar surface, into a PCR-style microtube, submerged in 20 µL of extraction solution and incubated in the thermocycler using the following protocol: 94 °C for 10 min, followed by 60 °C for 13 min and 10 °C for 15 min. After incubation, 20 µL of dilution solution were added, and the resulting mixture was vortexed for 2 min. Obtained DNA was used for the amplification of the ITS-rDNA region by PCR, using the fungal universal primer pair ITS1-F and ITS4 [56,57]. PCR reactions, consisting of a final amplification volume of 25 µL, with 12.5 µL of NZYTaq Green Master Mix (NZYTech™, Lisbon, Portugal), 1 µL of each primer (10 mM), 9.5 µL of ultra-pure water and 1 µL of template DNA, were performed using an ABI GeneAmp™ 9700 PCR System (Applied Biosystems, Waltham, MA, USA), with the following conditions: initial denaturation at 95 °C for 5 min, followed by 35 cycles of denaturation at 94 °C for 30 s, annealing at 52 °C for 30 s, and extension at 72 °C for 1 min, with a final extension at 72 °C for 8 min. Visual confirmation of the overall amplification of the ITS region was performed using agarose gel electrophoresis (1.2%) stained with GreenSafe Premium (NZYTech™, Lisbon, Portugal) and visualized in an Molecular Imager Bio-Rad Gel Doc XR™ (Bio-Rad, Hercules, CA, USA). Obtained amplicons were purified with the EXO/SAP Go PCR Purification Kit (GRISP, Porto, Portugal), following the manufacturer’s recommendations, and sequenced using an ABI 3730xl DNA Analyzer system (96 capillary instruments) at STABVIDA, Portugal. Obtained ITS sequences were analyzed using Chromas v.2.6.6 (Technelysium, Southport, QLD, Australia) and deposited in the GenBank database with the accession numbers: OP315718; OP315750–OP315755; OP315757–OP315759; OP315761; OP315763–OP315774; OP315776–OP315777; OP315779; OP315789–OP315792; OP339490; OP339492; OP359020; and OP381494.

Similarity searches were performed using the National Center of Biotechnology Information nucleotide database (NCBI's) basic local alignment search tool (BLAST), with the option standard nucleotide BLASTn of BLAST 2.6 [58]. Further confirmation of these results was performed using the online MycoBank database [59,60], with the molecular ID pairwise alignment tool (https://www.mycobank.org/page/Pairwise_alignment (accessed on 29 March 2022)) with the default parameters and all databases selected. To achieve a full agreement regarding species identification, molecular results were confirmed with an extensive macroscopic and microscopic analysis of taxonomic traits. Index Fungorum (www.indexfungorum.org (accessed on 30 March 2022)) and Mycobank (<https://www.mycobank.org/> (accessed on 30 March 2022)) [59,60] were consulted in order to provide the most accurate and correct taxonomic classification for each identified species.

To evaluate the diversity of cultivable fungal communities, the Species Richness (S), Shannon–Wiener index (H) and Species Evenness (E) were calculated using a PAST software package v.4.09, for each sample (L1, L2, L3 and L4). The re-isolation of the same species can occur from different samples and from different culture media plates, from the same sample. Therefore, to assess fungal populations in the four studied sites, the general isolation results were analyzed as species presence–absence for each sampling site regardless of the isolation method. A simple co-occurrence network between genera in the samples was constructed and visualized in the Cytoscape software (v.3.9.1, <http://www.cytoscape.org> (accessed on 12 July 2022)) [61]. A similar presence–absence evaluation scheme was performed to evaluate the different isolation media.

3. Results and Discussion

In the present study, we analyzed the fungal communities present in four samples collected from four distinct biodeterioration scenarios found in limestone tomb adornments in Lemos Pantheon of Trofa do Vouga. For that purpose, two different approaches were used, molecular high-throughput culture-independent methodologies in parallel with the traditional culture-dependent methodologies to complement their outputs and simultaneously tackle both techniques' limitations.

3.1. High-Throughput Sequencing Data Analysis

Fungal community composition analysis was assessed by sequencing ITS regions of the 18 S rRNA gene using the Illumina MiSeq[®] v3 platform. A total of 333,803 quality reads were recovered from all the samples and, at a 97% similarity cutoff level, grouped into 1588 operational taxonomic units (OTUs) at species level. The Good's Coverage index of all samples was over 99%, which indicated an adequate level of database coverage to identify most of the diversity in the samples. There were 612, 662, 833 and 270 OTUs identified in L1, L2, L3 and L4, respectively, and out of the total of observed OTUs, only 38 were shared among all four samples, which accounted for 2.4% of the total OTUs (Figure 3). These results point toward the presence of a higher number of distinctive populations associated with distinct biodeterioration patterns.

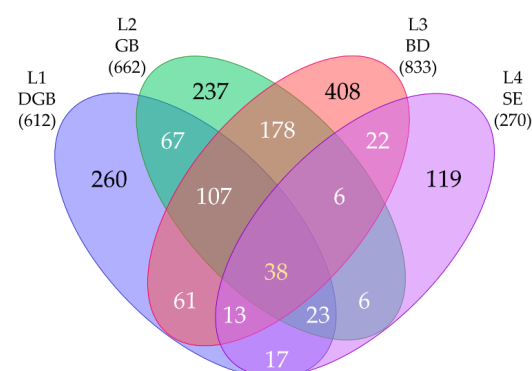


Figure 3. Venn diagram analysis of shared OTUs between samples.

The Chao 1, Abundance-based Coverage (ACE), Shannon (H), Gini–Simpson (1-D) and Dominance (D) indices were determined to quantify the Alpha diversity and understand the structure of the fungal community with respect to its richness (reflect the number of OTUs in samples) and evenness (reflect the distribution of abundances within OTUs). The greater the Chao or ACE index, the higher the expected species richness; the greater the H or 1-D indexes, the higher the diversity and the smaller the D, the higher the diversity. Analysis of Alpha diversity indices demonstrated a high fungal diversity in all four samples, with sample L1 presenting the greatest richness and diversity values and sample L3 the least, despite being the sample with the highest OTU count. Sample L1 also presented the lowest D value, indicating an even taxa distribution within this sampling point, in contrast with sample L3 exhibiting the highest D value suggesting the presence of a more prevalent taxon (or taxa). The detailed statistical data of α -diversity indexes are shown in Table 1.

Table 1. Richness and diversity statistical data generated from the metabarcoding analysis.

Sample ID	Reads	Good's Coverage	Observed OTU	Richness Estimator		Diversity Index		Dominance (D)
				Chao 1	ACE	Shannon (H)	Simpson (1-D)	
L1	93,237	99.96%	612	621	633	4.40	0.95	0.05
L2	99,703	99.86%	662	764	775	3.10	0.89	0.11
L3	130,788	99.93%	833	858	892	3.38	0.85	0.15
L4	10,075	99.80%	270	281	278	3.87	0.90	0.10

The OTUs were assigned to 7 phyla, 251 families and 500 genera, while only <1% of sequences were not assigned to any known phylum. At the phylum level, *Ascomycota* (accounting for 76.32% to 94.81%) and *Basidiomycota* (3.84% to 20.52%) were the two major fungal taxa across all samples. *Mortierellomycota* was the third most abundant phylum (>5% in L4) but, together with the phyla *Chytridiomycota* and *Glomeromycota*, was only detected in samples L1 and L4. *Rozellomycota* was present only in the L1 and L2 samples. The relative abundance of these last three phyla along with *Mucoromycota* was lower than 3% and differed across the samples. Figure 3 exhibits the relative abundance at the phylum level (Figure 4a), family level (Figure 4b) and genus level (Figure 4c). For the higher classification levels, only the 20 most abundant family and genera, considered individually for each sample, were discriminated in the graphs. Less abundant taxa were pooled and indicated as "Other".

The predominant families were *Cladosporiaceae* (25.9%), *Aspergillaceae* (7.5%), *Capnodiales_unclassified* (6.7%), *Saccharomycetales_fam Incertae sedis* (4.8%) and *Didymellaceae* (4.8%) in sample L1; *Cladosporiaceae* (26.3%), *Neodevriesiaceae* (18.3%), *Sordariomycetes_unclassified* (10.3%), *Cyphellophoraceae* (8.3%) and *Hypocreales_fam Incertae sedis* (5.6%) in sample L2; *Neodevriesiaceae* (40.5%), *Capnodiales_unclassified* (17.4%), *Cladosporiaceae* (8.4%), *Cordycipitaceae* (5.7%) and *Aspergillaceae* (5.3%) in sample L3; and *Capnodiales_unclassified* (34.5%), *Cordycipitaceae* (5.7%), *Nectriaceae* (5.6%), *Mortierellaceae* (5.3%) and *Eurotiomycetes_unclassified* 4.4% in sample L4.

The composition of the fungal community was further analyzed at the genus level. A total of 500 fungal genera were identified via taxonomic summary: 285 in sample L1; 251 in sample L2; 269 in sample L3; and 150 in sample L4. Of these 500 only 43 were common to all four spots, with samples L2 and L3 having the largest number of shared genera. Furthermore, genera were significantly different among samples, and L1 and L3 presented the greatest number of specific genera (Figure 5).

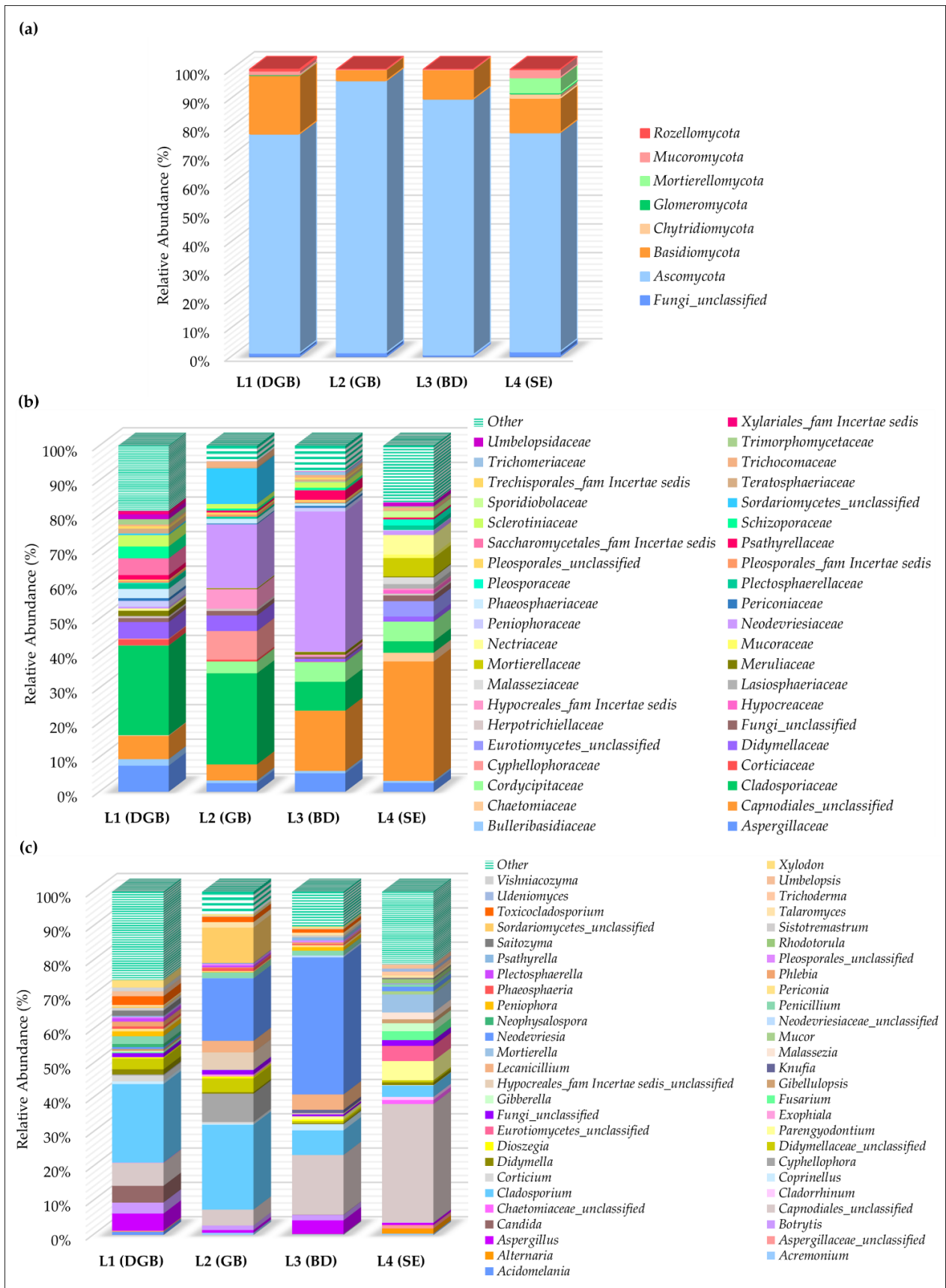


Figure 4. Relative abundance of the metabarcoding fungal diversity at (a) phylum, (b) family and (c) genus level per sample.

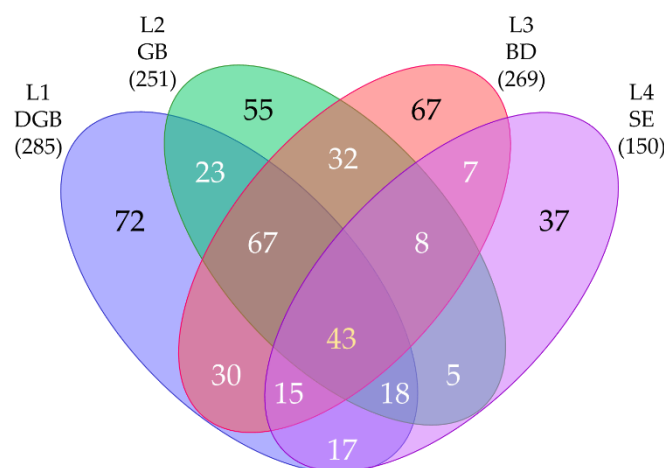


Figure 5. Venn diagram analysis of shared genera between samples.

The most dominant genera (relative abundance $\geq 1.5\%$) were *Cladosporium* (22.9%), *Capnodiiales_unclassified* (6.9%) and *Aspergillus* (4.9%), *Candida* (4.8%), *Botrytis* (3.2%), *Didymellaceae_unclassified* (3.1%), *Toxicocladosporium* (2.5%), *Penicillium* (2.3%), *Xylodon* (2.2%), *Corticium* (1.7%) and *Saitozyma* (1.5%) in L1; *Cladosporium* (24.7%), *Neodevriesia* (18.2%), *Sordariomycetes_unclassified* (10.3%), *Cyphellophora* (8.3%), *Hypocrales_fam_Incertae_sedis_unclassified* (5%), *Capnodiiales_unclassified* (4.6%), *Didymellaceae_unclassified* (4%), *Lecanicillium* (3.4%), *Penicillium* (1.7%), *Talaromyces* (1.6%) and *Toxicocladosporium* (1.5%) in L2; *Neodevriesia* (39.9%), *Capnodiiales_unclassified* (17.4%), *Cladosporium* (7.2%), *Lecanicillium* (4.5%), *Aspergillus* (4%), *Coprinellus* (1.7%) and *Botrytis* (1.6%) in L3; and *Capnodiiales_unclassified* (34.5%), *Parengyodontium* (5.6%), *Mortierella* (5.3%), *Eurotiomycetes_unclassified* (4.4%), *Cladosporium* (3.3%), *Fusarium* (2.5%), *Gibberella* (2.3%), *Malassezia* (1.9%) and *Alternaria* (1.5%) in L4.

Fungal communities differed among the studied samples, both in structure and taxonomic composition which supported our first hypothesis. These findings are consistent with the literature. Some of the 20 most abundant fungal genera detected in the present study, including *Alternaria*, *Aspergillus*, *Cladosporium*, *Corpinellus*, *Neophysalospora*, *Penicillium*, *Peniophora*, *Psathyrella* and *Udenomyces* had been previously reported in Ançã limestone through metabarcoding analysis [16]. Additionally, these results follow the same study, where it is stated that the Mycobiota associated with different biodeterioration types were taxonomically distinct, elucidating that different populations occur in distinct niches across similar lithology, denoting the importance and influence of microconditions in shaping these communities.

The distribution of the different communities (the 20 most abundant genera in each sample) can be observed in Figure 6. Specific taxa are clearly associated with the different samples (although not exclusively), suggesting a relationship between the present genera and the observed biodeterioration phenomena. The outlines with higher number of specific genera were SE (L4) and DGB (L1), for which the most relevant were: *Alternaria*, *Cladorrhinum*, *Fusarium*, *Malassezia*, *Mortierella*, *Mucor*, *Parengyodontium*, *Rhodotorula*, *Trichoderma* and *Udeniomyces* in L4; *Acidomelania*, *Candida*, *Corticium*, *Neophysalospora*, *Phlebia*, *Saitozyma*, *Vishniacozyma* and *Xylodon* in L1. In the other two settings, *Exophiala*, *Cyphellophora* and *Talaromyces* were prevalent in GB (L2) while *Knufia*, *Neodevriesia* and *Psathyrella* were more related to BD (L3).

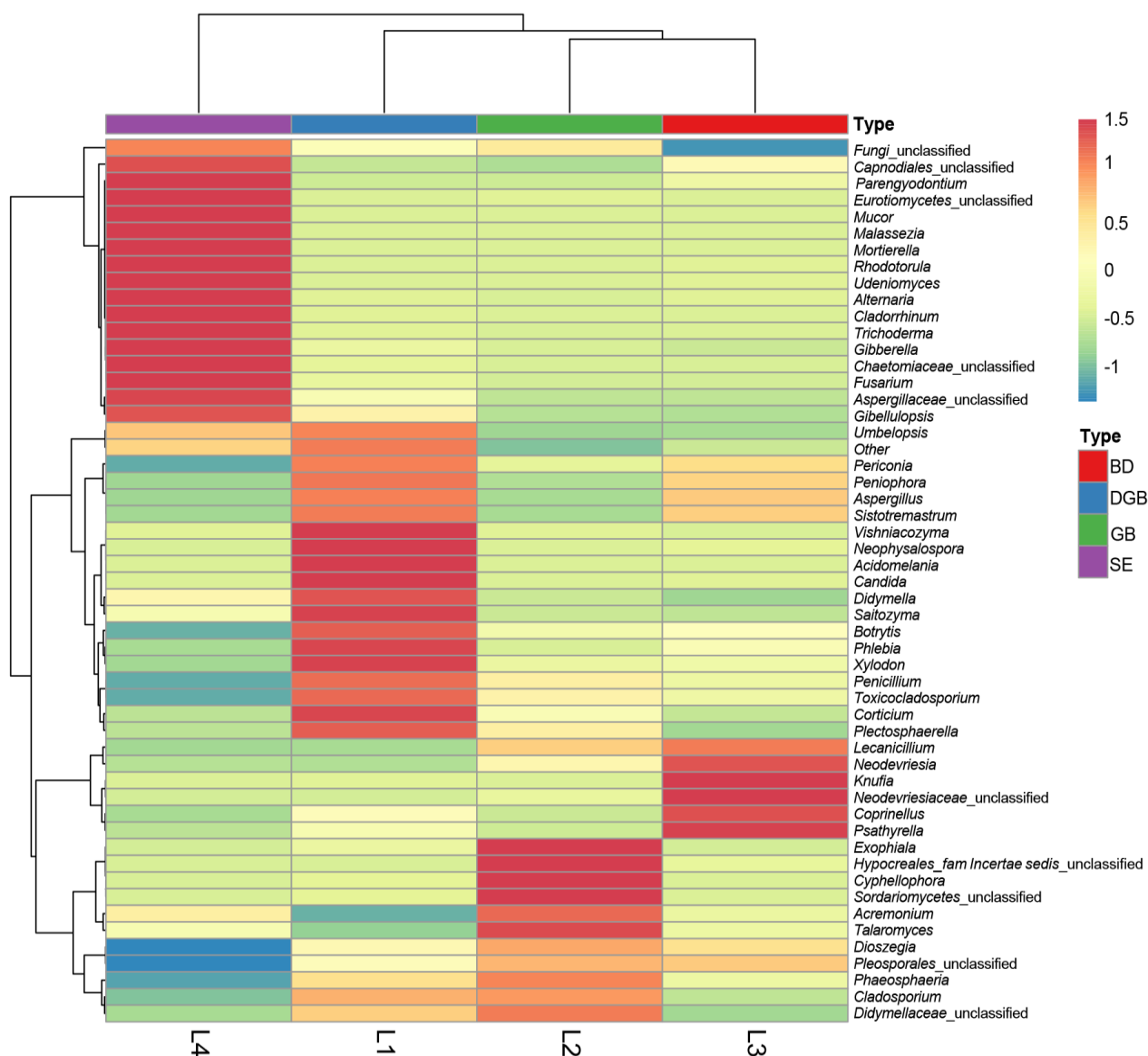


Figure 6. Heatmap representing the distinct distribution pattern of the 20 most abundant fungal genera across different biodeterioration types. Dark red color blocks represent a higher prevalence. Vertical clustering denotes the similarity in genera composition among samples. Horizontal clustering indicates the similarity of their abundance.

A β -diversity analysis was also performed. Principal coordinates analysis (PCoA) was used to explore and visualize similarities between the fungal communities present in each sample. Samples ordinated closer together have a greater similarity than those that are more distant. The PCoA results with Bray–Curtis distances at the genera level showed that samples from different biodeterioration patterns were not closely grouped together. Unweighted pair-group analysis (UPGMA) based on the relative abundance of fungal communities revealed a distinct clustering pattern between samples that originated from different biodeterioration patterns. Samples L2 and L3 were the most relatable in terms of genera composition; results agree with the Venn diagram and heatmap previously presented in Figures 5 and 6, respectively. Sample L1 was slightly more separated from L2 and L3, while sample L4 showed a strong separation from all the others (Figure 7a,b). This indicates that the compositions of fungal communities in these samples differ significantly from each other (PERMANOVA p -value < 0.005). The saline environment present in sample L4 was probably the major factor shaping this unique community.

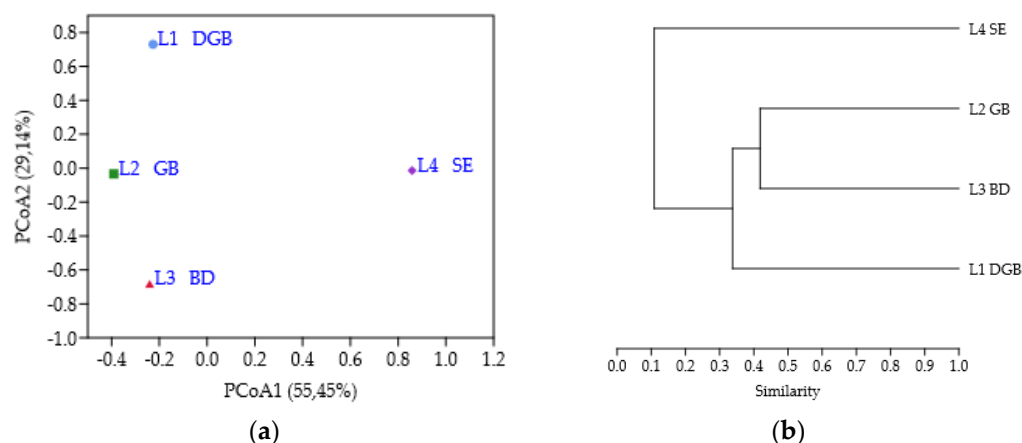


Figure 7. Depicting patterns of beta diversity for fungal communities in the different samples. (a) Principal coordinates analysis (PCoA) plot based on fungal genera composition. (b) UPGMA clustering analysis.

Through the SIMPER analysis, which calculates the contribution of each genus (%) to the dissimilarity between each two groups, we verified that *Neodevriesia* (20.15%) and *Cladosporium* (6.5%) were the genera that contributed the most to the dissimilarity between samples L1 and L2/L3. Regarding sample L4, *Capnodiales_unclassified* (17.5%), *Cladosporium* (9.74%) and *Parengyodontium* (3.1%) accounted for more than 30% of the total differentiation from L2/L3. The dissimilarity among samples L1 and L4 was mainly due to the high impact of *Capnodiales_unclassified* (15.34%), *Neodevriesia* (12.71%) and *Cladosporium* (5.7%). These results support the theory that specific population profiles were stratified by different biodeterioration patterns.

3.2. Diversity of the Culturable Fungi

The culture-dependent approach provided a good taxonomic resolution, resulting in a total of 135 isolates. Pure cultures were classified according to the observed characteristics of the colonies, and the representative fungal isolates were identified through amplification and sequencing of the ITS region of the rDNA. The morphological and molecular analyses led to the identification of 36 different species, together with 13 isolates for which a consensus on their identification was not attained (Table S1). Additionally, a few cultures of a filamentous actinobacteria of the genera *Streptomyces* were also isolated but not considered in the further analysis. Diversity indices are presented in Table 2.

Table 2. Diversity indices for cultivable fungal diversity.

Sample ID	Species Richness (S)	Shannon (H)	Evenness (e ^{-H/S})
L1	14	2.63	0.99
L2	15	2.35	0.70
L3	18	2.68	0.81
L4	6	1.53	0.77

Sample L3 revealed the highest species richness and Shannon index in contrast with sample L4 that presented the lowest. In turn, evenness was higher in L1, which indicates that the number of retrieved isolates from each species was more even in this sample. These are considerably different results from those obtained through metabarcoding.

Most of the isolated fungi belongs to phylum Ascomycota (>90%), with phylum Basidiomycota being detected only in sample L3, with 2 identified species, representing 5% of the total abundance for that sample. Figure 7 displays the overall abundance results at the family (Figure 8a) and species levels (Figure 8b).

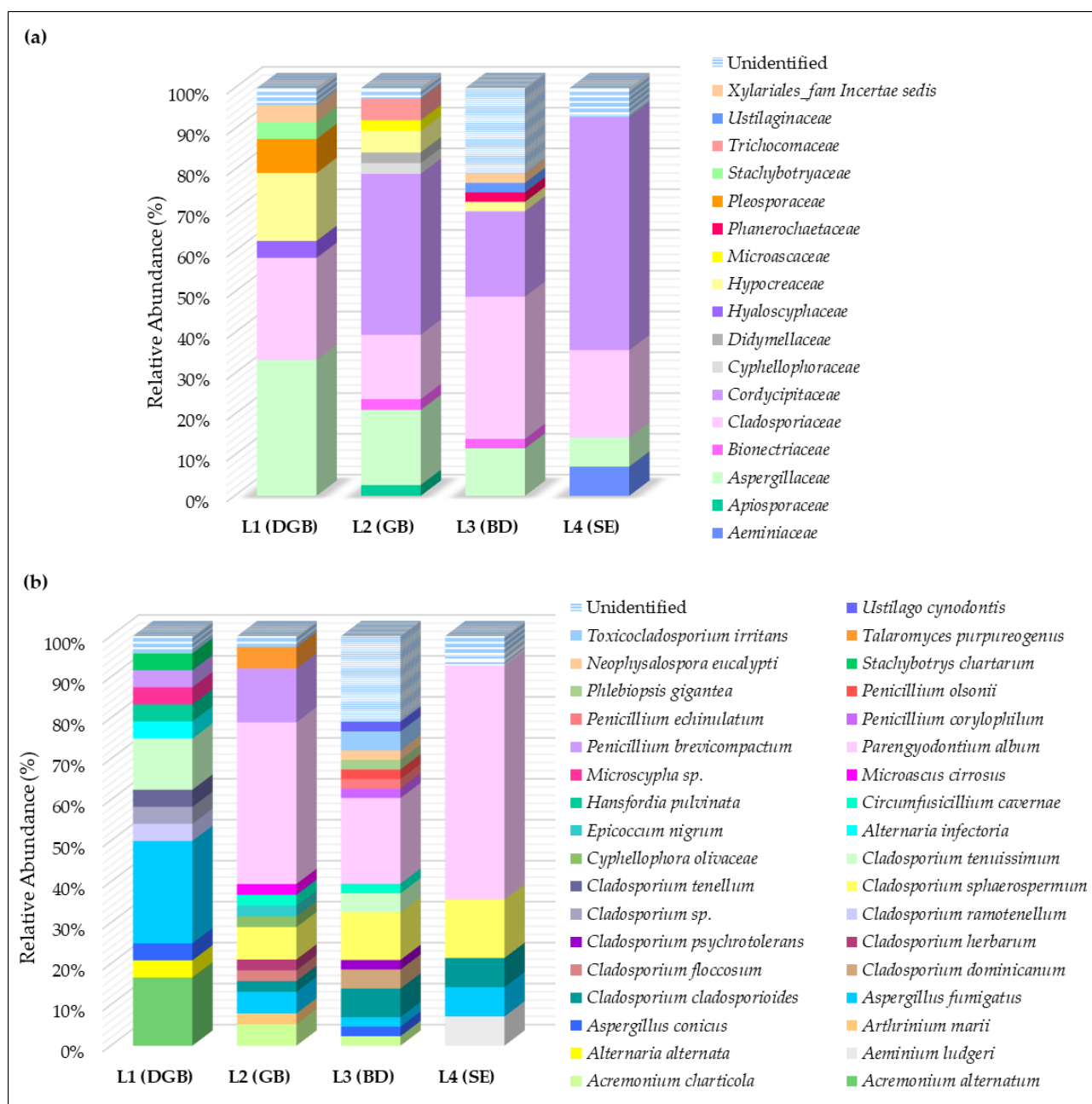


Figure 8. Relative abundance of the cultivable fungal diversity of all four sampling sites at (a) family level and (b) species level.

The predominant families were *Aspergillaceae* (33.3%), *Cladosporiaceae* (25%) and *Hypocreaceae* (16.7%) in sample L1; *Aspergillaceae* (18.4% and 11.6%), *Cladosporiaceae* (15.8% and 27.9%) and *Cordycipitaceae* (39.5% and 20.9%) in samples L2 and L3, respectively; and *Aeminiaceae* (14.3%), *Cladosporiaceae* (21.4%), *Cordycipitaceae* (57.1%) and *Aspergillaceae* (7.1%) in sample L4. Overall, the most common families across all samples were *Cladosporiaceae* and *Aspergillaceae*.

In general, the most frequently retrieved isolates were *Acremonium alternatum* (16.7%), *Aspergillus fumigatus* (25%), *Cladosporium tenuissimum* (12.5%) in sample L1; *Parengyodontium album* (39.5%) and *Penicillium brevicompactum* (13.2%) in sample L2; and *Cladosporium sphaerospermum* (11.6% and 14.3%) and *Parengyodontium album* (20.9% and 57.1%) in samples L3 and L4, respectively.

Due to the low match similarity and unique morphological characteristics, 13 isolates were not able to be identified to the species or genus level, and will require further inves-

tigation, as some may represent new taxa. The high degree of possible novelty and large variety of isolated fungi from a limited analyzed area of the rock surface point to a very rich and diverse pool of species in this habitat.

Through the ecological co-occurrence network analyses, it can be observed that most of the isolated species are specific to a distinctive biodeterioration pattern. Ten species were retrieved exclusively from DGB, seven from GB, 13 from BD and two from SE. BD had the highest number of exclusive (13) as well of shared (eight) species. Only *Aspergillus fumigatus* was present in all the biodeterioration scenarios (Figure 9).

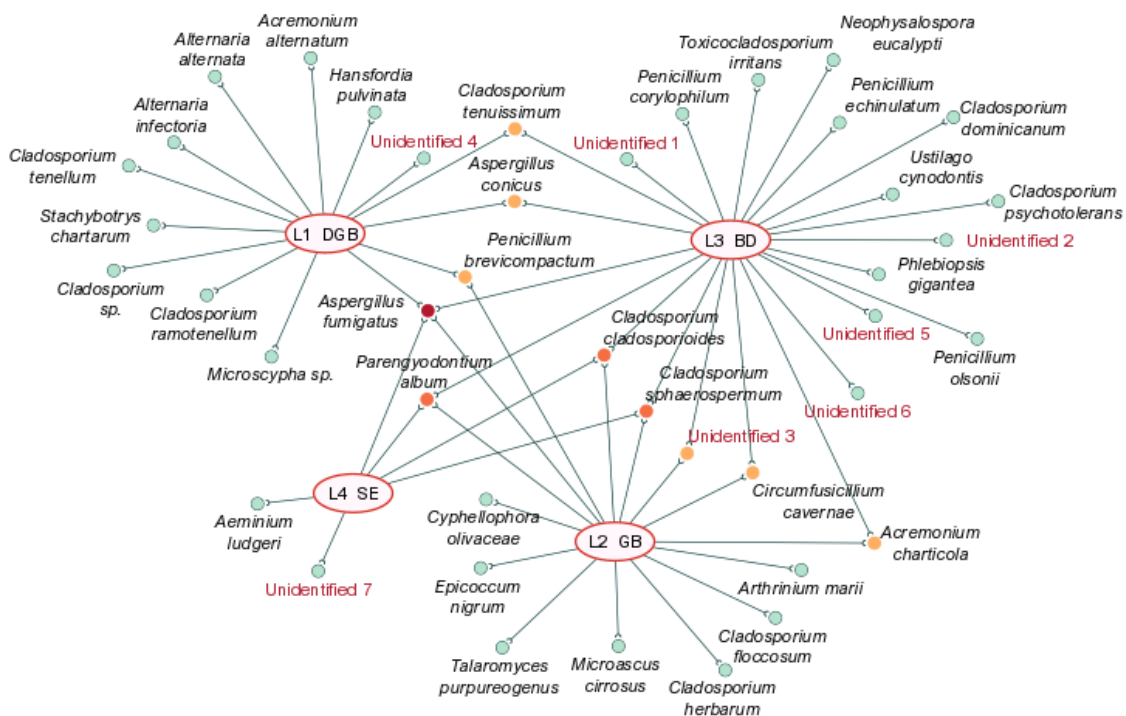


Figure 9. Network analysis showing the co-occurrence patterns of the cultivable species among sampling sites and their distinct biodeterioration patterns.

From the 36 identified species, *Acremonium alternatum*, *Arthrinium marii*, *Aspergillus conicus*, *Aspergillus fumigatus*, *Cladosporium dominicanum*, *Cladosporium floccosum*, *Cyphellophora olivaceae*, *Hansfordia pulvinata*, *Microascus cirrosus*, *Microscypha sp.*, *Neophysalospora eucalypti*, *Penicillium corylophilum*, *Penicillium echinulatum*, *Penicillium olsonii*, *Phlebiopsis gigantea*, *Stachybotrys chartarum*, *Talaromyces purpureogenus*, *Toxicocladosporium irritans* and *Ustilago cynodontis* are first reports, not only for Ançã limestone monuments, but for limestone monuments in general [37,62]. Additionally, this is the first time that *Aeminium ludgeri* and *Circumfusicillium cavernae*, two newly described species of Portuguese heritage, have been detected and isolated from a new different site (Figure S1) [63,64].

3.3. Influence of Culture Media on Species Richness

Regarding fungal cultivation, the different growth rates and nutrient requirements of different taxa are two key limiting factors [65]. To optimize our chances of recovering the greatest number of distinct species, but also to increase the likelihood of obtaining novel species, a total of six different culture media were used: standard PDA, a nutrient-rich generalist medium used for yeast and fungi isolation; DG-18, a selective medium for low water activity and xerophilic fungi; MEA supplemented with 10% NaCl (*w/v*), to facilitate the growth of halophilic fungi and some xerophilic species [66,67]; CZ used to isolate saprophytic fungi capable of utilizing sodium nitrate as the sole source of nitrogen; RB which helps to restrict the overgrowth of fast-growing strains, and also in the isolation of microcolonial fungi; and DSMZ 372-Halobacteria medium supplemented with 10%

NaCl (*w/v*) (HM 10%), which is useful in the isolation of microcolonial and halotolerant fungi [63].

Nutrient-rich media, such as PDA, tend to favor common fungal generalists that grow rapidly, often outgrowing more specialized species, and although they are commonly used, they are not suitable for the overall biodiversity analyses [68,69]. The importance of adding a wider variety of more selective culture media and prolonged incubation periods is that it provides an opportunity for slow growers and specialized species to develop and be detected [68,70,71].

Of the 123 fungal isolates recovered, the majority were obtained from DG18 (25%), followed by PDA (17%), CZ (16%), RB (15%), MEA NaCl 10% (15%) and lastly HM NaCl 10% (12%) (Figure 10). Additionally, DG18 provided the highest number of distinct taxa across all samples. These variations are determined according to their specific growth needs and demonstrate a high dominance of xerophilic species, distinguished by their ability to grow under conditions of low water activity. Only samples L2 and L3 had a wide range of distinct taxa isolated across all culture media, indicating a great versatility in the species present in those samples.

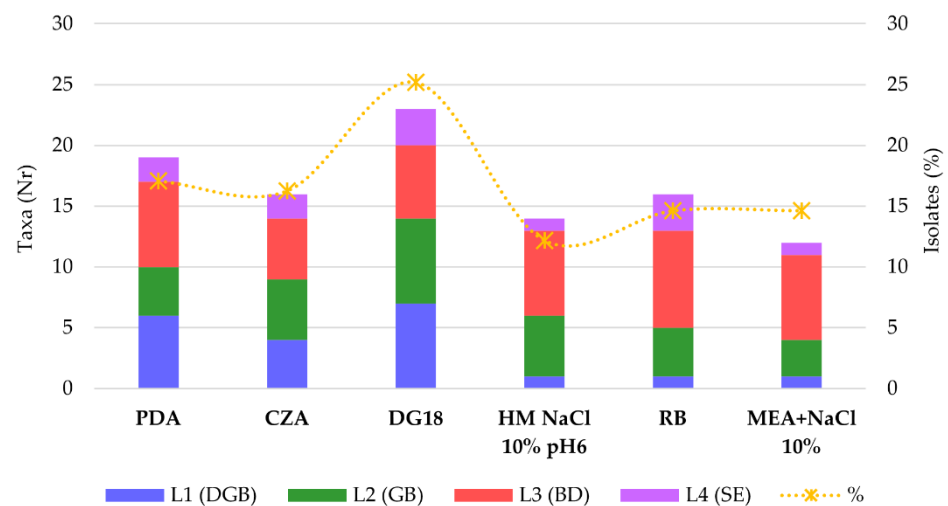


Figure 10. Number of different taxa and % of total isolates (same or different taxa) retrieved from each culture media.

Through a comparative analysis of the network results, showing the effect of each culture medium on the isolation of different species, it can be clearly observed that most species had a particular preference for a certain growth medium (Figure 11). Only *Parengyodontium album* and *Cladosporium sphaerospermum* were isolated in all six media. This result makes sense when we consider that both these species are globally distributed, highly ubiquitous and considered among the most common species found as indoor extremotolerant contaminants [72–74]. In addition, these species have been frequently reported as halotolerant and able to grow in multiple environments, including stone [75,76].

Other commonly retrieved species across different media are *C. cladosporioides*, *C. tenuissimum*, *Penicillium brevicompactum* and *Aspergillus fumigatus*.

The use of the high vs. selective nutrient approach to the cultivation of fungi resulted in a significantly different species composition being recovered from each media. Based on the presented species segregation throughout the different media, it is possible that culture methods could have been improved even further, with the introduction of new variables such as a wide range of growth temperatures, pH and osmotic concentrations, ultraviolet radiation exposure, among others, potentially enlarging the diversity of cultured microorganisms [77]. These results confirmed that the use of various culture media had a significant influence on the recovered species diversity. Furthermore, a greater number of unknown species (possibly novel taxa) were recovered from the selective media.

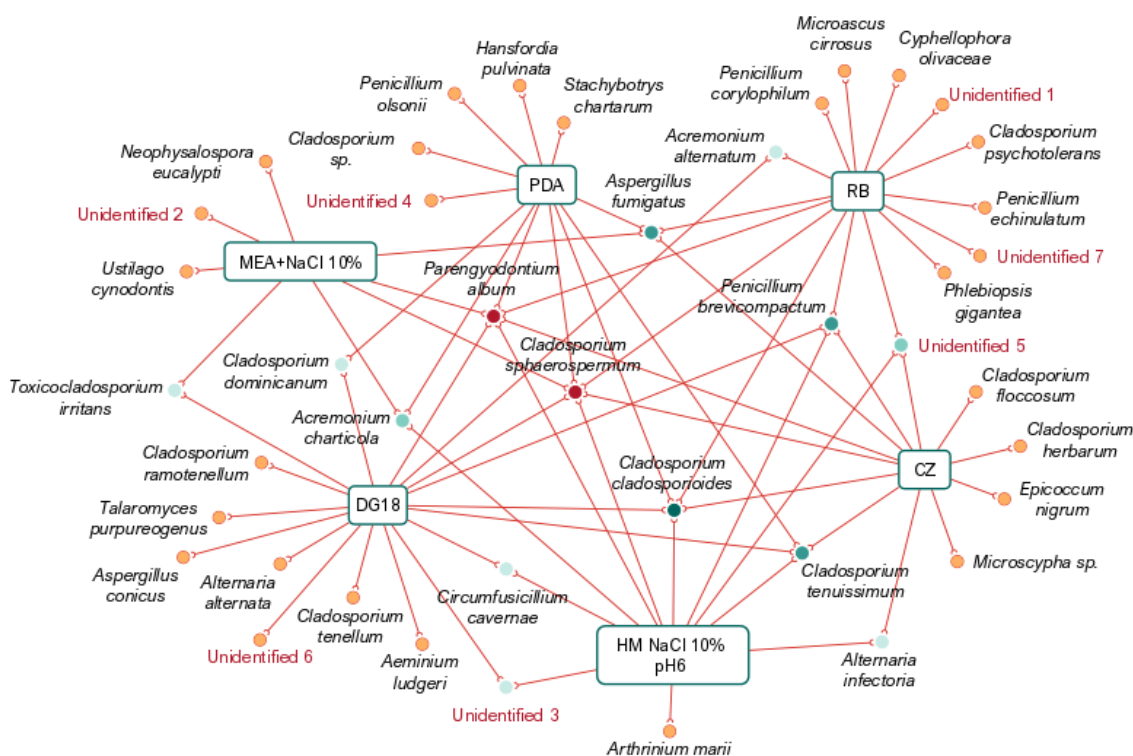


Figure 11. Co-occurrence network displaying the overlap of the cultivable species between the different culture media used for fungal isolation.

3.4. Mapping Biodeterioration Patterns

Ançã limestone is a homogenous and pure white limestone with a relatively high proportion of CaCO_3 (<96.5%), characterized by low compressive strength and hardness, high porosity (20–27.2%) and capillary absorption (10–14%). Due to its easy workability, it was extensively used in the decoration of the built patrimony, made famous for highly detailed carvings [37,78]. These are the same features that make it highly susceptible to fungal colonization and an exceptional target for biodeterioration. Similarly, parameters such as nutrient and water content and intensive diurnal and seasonal microclimatic oscillations to which stone is subjected, have a strong influence on the ability of fungi to colonize and grow in this substrate [79].

In general, microbial colonization initiates with a wide variety of phototrophic microorganisms, mainly cyanobacteria and algae [80–82]. The accumulation of photosynthetic biomass provides an excellent organic nutrient base, supporting the subsequent establishment and growth of heterotrophic communities [24,83]. In damper areas, such biofilms tend to be green [24,84], such as the ones found in samples L1 and L2 in this study. Both sampling points were located below the two main windows in Lemos Pantheon and biofilm development could be related to sunlight exposure and water infiltration due to poor insulation of the windows. Surface biofilms are embedded in extracellular polymeric substances (EPS), that act as a physical barrier that protects microorganisms, enabling the retention of water and minerals and maintaining a more stable temperature and humidity [83]. Such favorable conditions tend to hold a higher diversity.

However, the establishment of heterotrophic communities on rocks is possible even without the pioneering participation of phototrophic organisms and, according to Roeselers et al. [85], may in fact facilitate the subsequent growth of photosynthetic populations. In many cases, fungi are the first colonizers of stone surfaces [86,87], particularly rock black fungi, since they can survive and thrive in dry conditions, with a low requirement of nutrients and energy, and are less susceptible to seasonal variations [88]. Besides the aesthetic alterations, these fungi can induce a chemical deterioration. However, the most relevant damages are believed to be due to a mechanical action, causing a breakdown of

the stone matrix [89]. Our L3 sample, characterized by the presence of black discoloration, was the driest and darkest sampled spot with visible mineral disintegration, found behind one of the tomb chests.

The last sampling site (L4) was severely affected by salt damage. Salt decay is closely related to the petrophysical properties of stone, such as pore structure and other mechanical properties. Located near the Pantheon floor, due to capillary rise, water adsorption and condensation, probably from standard cleaning activities, favored efflorescence formation [90]. This precipitation process is a serious threat to the stone structure because salt occupying larger pores produces very high pressure, resulting in cracking, powdering, flaking, and material loss [91]. This salty micro-niche constitutes a suitable habitat for halophilic/halotolerant fungi, which, in conjunction with water impact, enhance the deterioration processes [92].

3.5. Metabarcoding vs. Culture-Dependent Diversity and Biodeterioration-Related Organisms

Regarding the metabarcoding fungal diversity obtained in the present study, our results show a strong dominance of the class *Dothideomycetes* in all samples, regardless of the biodeterioration pattern observed. Other classes such as *Sordariomycetes*, *Eurotiomycetes* and *Agaricomycetes* were also consistently present across all samples but in much lower abundance, with all classes belonging to *Ascomycota*. These results are consistent with the literature, with *Dothideomycetes* being one of the most frequent groups isolated from rocks [93–101].

Dothideomycetes are very diverse in term of species, encompassing morphologically and ecologically diverse fungi with different lifestyles and modes of nutrition. While many species are associated with plants (either as pathogens or as epiphytes), saprobic, coprophilous, lichen-forming and rock-inhabiting fungi are also present in this class [102]. The most common recovered fungal sequences in *Dothideomycetes* were composed of the orders *Capnodiales*, holding genera such as *Cladosporium*, *Toxicocladosporium*, and *Neodevriesia*, and *Pleosporales*, including the *Didymellaceae* family and *Alternaria*; however, abundance of these differed between samples. Along with the *Eurotiomycetes* genera frequently detected, such as *Aspergillus*, *Penicillium*, *Talaromyces* and *Cyphellophora*, most of these are generally widely distributed, highly ubiquitous and are considered among the most common genera found as indoor extremotolerant contaminants [18,28,73,76,77,102–105]. Members of the *Neodevriesiaceae* and *Cyphellophoraceae* include several species included in the rock inhabitant black fungi group, characterized as highly melanized and slow-growing organisms that are generally exceptionally skilled at exploiting most kinds of extremes environments [106–108].

In turn, *Sordariomycetes* is a very large class that comprises over 10,000 species that have been retrieved from a broad range of terrestrial and aquatic habitats, typically classified as saprobes, pathogens, and endophytes [109]. Integrated in this class, and also frequently detected in our metabarcoding analysis are *Fusarium* and *Parengyodontium*, often reported as associated with several different symptoms of deterioration in the cultural heritage [37,72], and *Lecanicillium*, which includes members that parasitize arthropods [110]. *Fusarium* and *Parengyodontium* were most abundant in sample L4, associated with salt efflorescence. The presence of entomopathogenic fungi may suggest that insects act as vectors in fungal dispersion to and from the walls in Lemos Pantheon [111].

Furthermore, salt efflorescence was the only biodeterioration outline where *Mortierella* (*Mortierellomycota*) was present, suggesting a halotolerant profile. Although the common lifestyle of these fungi is as soil inhabiting saprobic organisms on decaying organic matter, this genus has been previously reported in limestone [14].

Likewise, *Botrytis* (*Leotiomycetes*) is a widespread saprophyte as well as plant pathogen, but frequently detected in limestone and present across all biodeterioration scenarios. These results are coherent with its known halotolerant nature and suggest a possible xerophilic adaptation [14,16].

Corticium, *Xylodon* and *Coprinellus* (*Agaricomycetes*) are saprotroph fungi belonging to *Basidiomycota* [112–114]. The first two genera are found mainly associated with green biofilms, while *Coprinellus* was present in all four locations, especially in black discoloration (L3), possibly indicating a more xerophilic and halotolerant profile.

Moreover, *Candida* (*Ascomycota*, *Saccharomycetes*), *Malassezia* (*Basidiomycota*, *Malasseziales*) and *Saitozyma* (*Basidiomycota*, *Tremellomycetes*) are yeast-like fungi, being the first two opportunistic parasites in human and other warm-blooded animals [115,116], whereas *Saitozyma* is commonly found in soil and plants [117,118]. In a study conducted in the Morassina cave [119], where the yeast genus *Candida* has been identified, reference was made to its ability to grow under acidic conditions.

Finally, a greater number of distinctive specific taxa associated with the different types of biodeterioration observed were mainly present in the fractions with lower abundances. While green biofilms had a very rich and diverse populations composition, a black discoloration outline (L3) was highly dominated by *Capnodiales* (~70%), particularly *Neodevriesiaceae* (~40%), *Cladosporiaceae* and unclassified *Capnodiales*, demonstrating the high prevalence of black fungi. The salt efflorescence was the most unique scenario, characterized by the presence of distinct phyla such as *Mortierellomycota*, *Glomeromycota* and *Chytridiomycota*. Unclassified *Capnodiales* (~30%) was also markedly present in this sampling point.

When considering the HTS data, highly abundant taxa did not always belong to well-known taxonomic groups, but additionally to unidentified lineages. Therefore, we can hypothesize that species richness within those, particularly *Dothideomycetes*, *Eurotiomycetes* and *Sordariomycetes*, remains woefully underestimated, and that many taxa previously unknown are present within, highlighting the need for further studies, especially for fungi colonizing rocky substrates.

In addition, generalized studies of community diversity by molecular methods alone lack the discrimination between living and dead material, or active and dormant organisms. As a result, molecular profiling can be expected to provide different results from those obtained from culture isolation techniques. Combining molecular techniques with a more classical approach may allow a much greater understanding of fungal communities.

Concerning the cultivable diversity, differences between the fungal profiles obtained by isolation and metabarcoding were noted. With the exception of *Alternaria*, *Aspergillus*, *Cladosporium*, *Cyphellophora*, *Parengyodontium*, *Penicillium*, *Talaromyces* and *Toxicocladosporium*, some of the most abundant taxa in the metabarcoding approach were absent from the fungi identified by culture-based methods. This was the case for *Fusarium*, *Mortierella* and *Botrytis*, for example, all of which were previously isolated from the stone and are fast-growing and easy to culture. *Neodevriesia*, despite being particularly abundant in samples L2 and L3, is a slow-growing and weak competitive black fungi, therefore being difficult to isolate. Nonetheless, a very large number of strains from different genera (e.g., *Neophysalospora*, *Epicoccum*, *Stachybotrys*, *Acremonium* and *Phlebiopsis*) were isolated, despite their low proportions in the metabarcoding analysis. Additionally, *Arthrinium*, *Microascus*, *Microscypha*, *Ustilago*, *Aeminiium* and *Circumfusicillium* were not detected at all through the metabarcoding analysis.

The detection by cultivation of numerous taxa that go undetected in metagenomic studies is far from insignificant, even if these microorganisms are in low abundance. This may be verified because these species go under unidentified groups in HTS analysis or are present below the detection thresholds of large-scale molecular studies, demonstrating a major “depth bias” of the metagenomic approaches.

Metabarcoding proved insufficient on its own, and isolation provided an added value for the accurate characterization of the complex fungal community found on limestone. Therefore, for a more complete and thorough characterization, the use of both approaches is probably the best solution. In fact, one of the main advantages of culture isolation is that the different organisms can be preserved for further testing, to understand their ecological functions and identify specific interactions with materials and other organisms. Furthermore,

only with isolation can new strains be obtained for further characterization and description, enhancing our current knowledge of the true diversity of fungi. Similar conclusions have been recently reported by Selbmann et al. [120] in a study that compared culture-dependent and amplicon sequencing approaches of black fungi in Antarctic cryptoendolithic communities, where their results also sustain the theory that the application of both approaches is desirable to discern microbial diversity and community structure in deeper detail, since the respective limits are complementary. Furthermore, in a new publication, Chen and Gu [121] also suggest that the analysis of the microbial community by HTS should be further improved using RNA-based cDNA, to verify the metabolically active population present in a sample, revealing a more meaningful community composition and structure.

Fungal mediated biodeterioration is related to: discoloration caused by pigments released from, or contained within, the microorganism (aesthetic action); biocorrosion of the mineral support by acidolysis and oxidoreductive processes generated by metabolism (biochemical action); and physical damage caused by the mechanical action of the biomass colonizing the material during its growth (physical action) that leads to the disruption of the material or to its distortion [32].

From the isolated species, *Aspergillus fumigatus*, *Epicoccum nigrum*, *Talaromyces purpureogenus*, *Alternaria* spp. and *Cladosporium* spp., and highly melanized black fungi such as *Aeminiium ludgeri* and *Cyphellophora olivaceae* are known pigment producers, and therefore their growth contributes to aesthetic alterations [24,26,29,122].

Moreover, *Alternaria infectoria* and black fungi are also known to contribute to stone biopitting through physical action, triggered by disaggregation of rock grains determined by the internal pressure caused by hyphae penetrating stone [26,123].

Among biochemical mechanisms induced by fungal metabolism, the production of inorganic acids (e.g., nitric, sulfuric, and carbonic) and organic acids (e.g., oxalic, citric, gluconic, malic, etc.) represents a significant part in biodeterioration processes [24]. *Aspergillus fumigatus*, *Epicoccum nigrum*, *Penicillium brevicompactum* and *Penicillium corylophilum* are known producers of oxalic acid. Oxalate is a key fungal metabolite and considered one of the most important in terms of its role in biodeterioration, biocorrosion and bioweathering, often associated with fungal-mediated rock and mineral transformations, that seems ubiquitous in the context of biodeterioration [124]. Other acid-producing species isolated in this study include *Alternaria alternata* (tenuazonic acid), *Cladosporium tenuissimum* (formic, fumaric, gluconic and lactic acids), *Epicoccum nigrum* (acetic, butyric, citric, fumaric, malic and succinic acids) and *Penicillium brevicompactum* (citric, fumaric and gluconic acids). Due to the acid-producing nature of the above species, they likely contribute to the acidification and dissolution of limestone minerals [14,125]. Additionally, fungal species with known CaCO₃ dissolution abilities, such as *Acremonium charticola*, *Cladosporium sphaerospermum*, *Cyphellophora olivacea*, *Parengyodontium album* and *Penicillium brevicompactum*; and mineralization or crystallization abilities, such as *Aeminiium ludgeri*, *Alternaria alternata*, *Alternaria infectoria*, *Cladosporium cladosporioides*, *Cladosporium sphaerospermum*, *Epicoccum nigrum* and *Penicillium brevicompactum* [62], have also been retrieved in this study.

Despite bacteria not being an object of this study, the frequent isolation of a filamentous *Actinobacteria* was an interesting result. Some organisms from this phylum (e.g., *Streptomyces*) have been associated with damaged limestone, frequently promoting a decrease in pH, therefore working as biodegradation phenomena indicators [24,126].

4. Conclusions

Cultural heritage, such as stone monuments, connects people with their past history and enriches us with cultural values, making it imperative to preserve and conserve its messages and intrinsic values. Stone biodeterioration is a key challenge. The identification and study of microbial communities and possible outbreaks, as well as their contribution to this process, is crucial knowledge to formulate effective conservation strategies to prevent biodeterioration and create effective and well-planned restoration plans.

The data obtained in this work provide an important insight to fully understand the fungal diversity and its distribution across dissimilar biodeterioration outlines in limestone, highlighting the importance of a case-by-case approach, since material transformation is context-specific. This study also revealed that, despite HTS being a powerful tool in exploring largely diverse environments when compared with traditional cultivation methodologies, each approach tends to capture different community fractions. Our results demonstrate that through HTS we were able to characterize the diversity and abundance of the complex fungal communities present in different bio-deterioration outlines in great detail, but several genera that were successfully isolated were not detected by this approach. On the other hand, with classic culture techniques for fungal isolation, we found only a few shared genera detected when both approaches were applied. The overlap and considerable differences in fungal community detected by both approaches highlight their complementarity, and their combination generates more detailed information when profiling these communities. Additionally, regardless of the fact that the culture-dependent approach lacks the resolution needed to distinguish the complexity of communities' composition, it gave us a chance to visualize and preserve cultures to further test their functions, study their genetics and genomics, explore their environmental requirements and test cleaning agents and biocides, key information to prevent and/or control future outbreaks and consequent biodeterioration. In addition, it was proved that the use of a wide variety of selective culture media positively influenced the great diversity of cultivable fungi obtained in this study. Finally, this study also contributes significantly to the inventory of stone-colonizing fungal diversity.

Supplementary Materials: The following supporting information can be downloaded at <https://www.mdpi.com/article/10.3390/app122010650/s1>, Table S1: Identification of all fungal isolates retrieved in this study. Figure S1: Isolates of two newly described species (a) *Circumfusicillium cavernae* (*Bionectriaceae*), (b) *C. cavernae* colony in detail and (c) *Aeminium ludgeri* (*Aeminiaceae*), (d) *A. ludgeri* colony appearance after starting maturing, on PDA, first described in deteriorated limestone in Coimbra (Portugal) and isolated in the present study [64,65].

Author Contributions: Conceptualization, D.S.P., N.M., I.T. and A.P.; Methodology, D.S.P., J.T. and A.P.; Software, D.S.P. and L.F.; Validation, D.S.P., N.M., I.T. and A.P.; Formal analysis, D.S.P.; Investigation, D.S.P.; Resources, N.M., I.T. and A.P.; Data Curation, D.S.P.; Writing—Original Draft Preparation, D.S.P.; Writing—Review and Editing, D.S.P., L.F., J.T., N.M., I.T. and A.P.; Visualization, D.S.P.; Supervision, N.M., I.T. and A.P.; Project Administration, A.P.; Funding Acquisition, A.P. All authors have read and agreed to the published version of the manuscript.

Funding: Diana Paiva was supported by a PhD research grant (UI/BD/150843/2021) awarded by the Centre for Functional Ecology—Science for People & the Planet (CFE) and co-funded by Fundação para a Ciência e Tecnologia, I.P. (FCT) through national funding by the Ministério da Ciência, Tecnologia e Ensino Superior (MCTES) from Fundo social Europeu (FSE). This work was carried out in the R&D Unit Centre for Functional Ecology—Science for People & the Planet (CFE), with reference UIDB/04004/2020, financed by FCT/MCTES through national funds (PIDDAC).

Institutional Review Board Statement: Not applicable.

Informed Consent Statement: Not applicable.

Data Availability Statement: All relevant data are presented in the paper and its Supporting Information Files. Metagenomic data were deposited in the NCBI SRA database under the reference PRJNA875387. The nucleotide sequences were deposited in the GenBank database under accession numbers: OP315718; OP315750–OP315755; OP315757–OP315759; OP315761; OP315763–OP315774; OP315776–OP315777; OP315779; OP315789–OP315792; OP339490; OP339492; OP359020; and OP381494.

Acknowledgments: The authors would like to thank the Trofa's Administration Parish Council for granting us permission to access the Lemos Pantheon, and to Father José Luís Pimenta, Parish Priest of the Church of Trofa do Vouga which houses the Lemos Pantheon, who kindly received

us and supervised the collection of samples used in this research as well as for providing valuable information about the monument's history.

Conflicts of Interest: The authors declare no conflict of interest.

References

1. Aires-Barros, L. As Rochas dos Monumentos Portugueses. In *Tipologias e Patologias*; Instituto Português do Património Arquitectónico (IPPAR): Lisbon, Portugal, 2001.
2. Aires-Barros, L. Património Cultural Construído: Algumas notas para o seu estudo e preservação. *PedraCal* **2002**, *13*, 11–14. Available online: http://www.gecorpa.pt/Upload/Revistas/Rev13_Pag11.pdf (accessed on 4 June 2022).
3. Gadd, G.M. Fungi, Rocks, and Minerals. *Elements* **2017**, *3*, 171–176. [[CrossRef](#)]
4. McNamara, C.J.; Mitchell, R. Microbial Deterioration of Historic Stone. *Front. Ecol. Environ.* **2005**, *3*, 445–451. [[CrossRef](#)]
5. Griffin, P.S.; Indictor, N.; Koestler, R.J. The biodeterioration of stone: A review of deterioration mechanisms, conservation case histories, and treatment. *Int. Biodeterior. Biodegrad.* **1991**, *28*, 187–207. [[CrossRef](#)]
6. Warscheid, T.; Braams, J. Biodeterioration of stone: A review. *Int. Biodeterior. Biodegrad.* **2000**, *46*, 343–368. [[CrossRef](#)]
7. Gaylarde, C.; Ribas Silva, M.; Warscheid, T. Microbial impact on building materials: An overview. *Mater. Struct.* **2003**, *36*, 342–352. [[CrossRef](#)]
8. Crispim, C.A.; Gaylarde, C.C. Cyanobacteria and biodeterioration of cultural heritage: A review. *Microb. Ecol.* **2005**, *49*, 1–9. [[CrossRef](#)] [[PubMed](#)]
9. Macedo, M.F.; Miller, A.Z.; Dionísio, A.; Saiz-Jimenez, C. Biodiversity of cyanobacteria and green algae on monuments in the Mediterranean Basin: An overview. *Microbiology* **2009**, *155*, 3476–3490. [[CrossRef](#)] [[PubMed](#)]
10. Gaylarde, C.C.; Gaylarde, P.M.; Neilan, B.A. Endolithic phototrophs in built and natural stone. *Curr. Microbiol.* **2012**, *65*, 183–188. [[CrossRef](#)]
11. Keshari, N.; Adhikary, S.P. Diversity of cyanobacteria on stone monuments and building facades of India and their phylogenetic analysis. *Int. Biodeterior. Biodegrad.* **2014**, *90*, 45–51. [[CrossRef](#)]
12. Unković, N.; Dimkić, I.; Stupar, M.; Stanković, S.; Vukojević, J.; Grbić, M.L. Biodegradative potential of fungal isolates from sacral ambient: In vitro study as risk assessment implication for the conservation of wall paintings. *PLoS ONE* **2018**, *13*, e0190922. [[CrossRef](#)]
13. Soares, F.; Portugal, A.; Trovão, J.; Coelho, C.; Mesquita, N.; Pinheiro, A.C.; Gil, F.; Catarino, L.; Cardoso, S.M.; Tiago, I. Structural diversity of photoautotrophic populations within the UNESCO site ‘Old Cathedral of Coimbra’ (Portugal), using a combined approach. *Int. Biodeterior. Biodegrad.* **2019**, *140*, 9–20. [[CrossRef](#)]
14. Trovão, J.; Portugal, A.; Soares, F.; Paiva, D.S.; Mesquita, N.; Coelho, C.; Pinheiro, A.C.; Catarino, L.; Gil, F.; Tiago, I. Fungal diversity and distribution across distinct biodeterioration phenomena in limestone walls of the old cathedral of Coimbra, UNESCO World Heritage Site. *Int. Biodeterior. Biodegrad.* **2019**, *142*, 91–102. [[CrossRef](#)]
15. Trovão, J.; Tiago, I.; Catarino, L.; Gil, F.; Portugal, A. In vitro analyses of fungi and dolomitic limestone interactions: Bioreceptivity and biodeterioration assessment. *Int. Biodeterior. Biodegrad.* **2020**, *155*, 105107. [[CrossRef](#)]
16. Trovão, J.; Gil, F.; Catarino, L.; Soares, F.; Tiago, I.; Portugal, A. Analysis of fungal deterioration phenomena in the first Portuguese King tomb using a multi-analytical approach. *Int. Biodeterior. Biodegrad.* **2020**, *149*, 104933. [[CrossRef](#)]
17. Trovão, J.; Soares, F.; Tiago, I.; Catarino, L.; Portugal, A.; Gil, F. A contribution to understand the Portuguese emblematic Anã limestone bioreceptivity to fungal colonization and biodeterioration. *J. Cult. Herit.* **2021**, *49*, 305–312. [[CrossRef](#)]
18. Coelho, C.; Mesquita, N.; Costa, I.; Soares, F.; Trovão, J.; Freitas, H.; Portugal, A.; Tiago, I. Bacterial and Archaeal Structural Diversity in Several Biodeterioration Patterns on the Limestone Walls of the Old Cathedral of Coimbra. *Microorganisms* **2021**, *9*, 709. [[CrossRef](#)] [[PubMed](#)]
19. Mohammadi, P.; Krumbein, W. Biodeterioration of Ancient Stone Materials from the Persepolis Monuments (Iran). *Aerobiologia* **2008**, *24*, 27–33. [[CrossRef](#)]
20. Papida, S.; Murphy, W.; May, E. Enhancement of physical weathering of building stones by microbial populations. *Int. Biodeterior. Biodegrad.* **2000**, *46*, 305–317. [[CrossRef](#)]
21. Gadd, G.M. Geomicrobiology of the built environment. *Nat. Microbiol.* **2017**, *2*, 16275. [[CrossRef](#)]
22. Miletto, M.; Lindow, S.E. Relative and contextual contribution of different sources to the composition and abundance of indoor air bacteria in residences. *Microbiome* **2015**, *3*, 61. [[CrossRef](#)] [[PubMed](#)]
23. Dedesko, S.; Siegel, J.A. Moisture parameters and fungal communities associated with gypsum drywall in buildings. *Microbiome* **2015**, *3*, 71. [[CrossRef](#)] [[PubMed](#)]
24. Scheerer, S.; Ortega-Morales, O.; Gaylarde, C. Chapter 5 Microbial Deterioration of Stone Monuments—An Updated Overview. *Adv. Appl. Microbiol.* **2009**, *66*, 97–139. [[CrossRef](#)] [[PubMed](#)]
25. Dakal, T.C.; Cameotra, S.S. Microbially induced deterioration of architectural heritages: Routes and mechanisms involved. *Environ. Sci. Eur.* **2012**, *24*, 36. [[CrossRef](#)]
26. Sterflinger, K. Fungi: Their role in deterioration of cultural heritage. *Fungal Biol. Rev.* **2010**, *24*, 47–55. [[CrossRef](#)]
27. Sterflinger, K.; Piñar, G. Microbial deterioration of cultural heritage and works of art—Tilting at windmills? *Appl. Microbiol. Biotechnol.* **2013**, *97*, 9637–9646. [[CrossRef](#)]

28. Gadd, G.M. Geomycology: Biogeochemical transformations of rocks, minerals, metals and radionuclides by Fungi, Bioweathering and Bioremediation. *Mycol. Res.* **2007**, *111*, 3–49. [[CrossRef](#)] [[PubMed](#)]
29. Sterflinger, K. Fungi as geologic agents. *Geomicrobiol. J.* **2000**, *17*, 97–124. [[CrossRef](#)]
30. González, J.M.; Sáiz-Jiménez, C. Application of molecular nucleic acid-based techniques for the study of microbial communities in monuments and artworks. *Int. Microbiol.* **2005**, *8*, 189–194. [[PubMed](#)]
31. Dakal, T.C.; Arora, P.K. Evaluation of potential of molecular and physical techniques in studying biodeterioration. *Rev. Environ. Sci. Bio/Technol.* **2012**, *11*, 71–104. [[CrossRef](#)]
32. Mihajlovski, A.; Seyer, D.; Benamara, H.; Bousta, F.; Di Martino, P. An overview of techniques for the characterization and quantification of microbial colonization on stone monuments. *Ann. Microbiol.* **2015**, *65*, 1243–1255. [[CrossRef](#)]
33. Sanmartín, P.; DeAraujo, A.; Vasanthakumar, A. Melding the Old with the New: Trends in Methods Used to Identify, Monitor, and Control Microorganisms on Cultural Heritage Materials. *Microb. Ecol.* **2018**, *76*, 64–80. [[CrossRef](#)] [[PubMed](#)]
34. Otlewska, A.; Adamiak, J.; Gutarowska, B. Application of molecular techniques for the assessment of microorganism diversity on cultural heritage objects. *Acta Biochim. Pol.* **2014**, *61*, 217–225. [[CrossRef](#)] [[PubMed](#)]
35. Goodwin, S.; McPherson, J.D.; McCombie, W.R. Coming of age: Ten years of next-generation sequencing technologies. *Nat. Rev. Genet.* **2016**, *17*, 333–351. [[CrossRef](#)] [[PubMed](#)]
36. Castro, A.P.; Sartori da Silva, M.R.S.; Quirino, B.F.; Kruger, R.H. Combining “omics” strategies to analyze the biotechnological potential of complex microbial environments. *Curr. Protein Pept. Sci.* **2013**, *14*, 447–458. [[CrossRef](#)]
37. Pinheiro, A.C.; Mesquita, N.; Trovão, J.; Soares, F.; Tiago, I.; Coelho, C.; Carvalho, H.P.; Gil, F.; Catarino, L.; Piñar, G.; et al. Limestone biodeterioration: A review on the portuguese cultural heritage scenario. *J. Cult. Herit.* **2019**, *36*, 275–285. [[CrossRef](#)]
38. Ettenauer, J.; Piñar, G.; Tafer, H.; Sterflinger, K. Quantification of fungal abundance on cultural heritage using real time PCR targeting the β -actin gene. *Front. Microbiol.* **2014**, *5*, 62. [[CrossRef](#)]
39. Panteão dos Lemos. Available online: <https://www.cm-agueda.pt/visite/turismo/a-visitar/patrimonio/panteao-dos-lemos> (accessed on 22 August 2022).
40. Restauo “Exemplar” da Igreja Matriz da Trofa Valoriza Património. Available online: <https://www.jb.pt/2022/08/restauo-exemplar-da-igreja-matriz-da-trofa-valoriza-patrimonio/> (accessed on 22 August 2022).
41. Doehne, E.; Price, C.A. *Stone Conservation: An Overview of Current Research*, 2nd ed.; The Getty Conservation Institute: Los Angeles, CA, USA, 2010; pp. 29–32.
42. Douglas-Jones, R.; Hughes, J.J.; Jones, S.; Yarrow, T. Science, value and material decay in the conservation of historic environments. *J. Cult. Herit.* **2016**, *21*, 823–833. [[CrossRef](#)]
43. Igreja Paroquial de Trofa/Igreja de São Salvador e Panteão dos Lemos. Available online: http://www.monumentos.gov.pt/Site/APP_PagesUser/SIPA.aspx?id=1042 (accessed on 22 August 2022).
44. Vergès-Belmin, V. ICOMOS-ISCS: *Illustrated glossary on stone deterioration patterns Glossaire illustré sur les formes d’altération de la pierre*; ICOMOS-MONUMENTS and SITES XV: Paris, France, 2008; ISBN 978-2-918086-00-0.
45. Tedersoo, L.; Bahram, M.; Põlme, S.; Kõljalg, U.; Yorou, N.S.; Wijesundera, R.; Ruiz, L.V.; Vasco-Palacios, A.M.; Thu, P.Q.; Suija, A.; et al. Global diversity and geography of soil fungi. *Science* **2014**, *346*, 1256688. [[CrossRef](#)] [[PubMed](#)]
46. ILLUMINA, Inc. 16S Metagenomic Sequencing Library Preparation. Preparing 16S Ribosomal RNA Gene Amplicons for the Illumina MiSeq System. 2013. Available online: https://support.illumina.com/downloads/16s_metagenomic_sequencing_library_preparation.html (accessed on 3 January 2022).
47. Comeau, A.M.; Douglas, G.M.; Langille, M.G.I. Microbiome helper: A custom and streamlined workflow for microbiome research. *mSystems* **2017**, *2*, e00127-16. [[CrossRef](#)] [[PubMed](#)]
48. Schmieder, R.; Edwards, R. Quality control and preprocessing of metagenomic datasets. *Bioinformatics* **2011**, *27*, 863–864. [[CrossRef](#)]
49. Schubert, M.; Lindgreen, S.; Orlando, L. Adapter Removal v2: Rapid adapter trimming, identification, and read merging Findings Background. *BMC Res. Notes* **2016**, *9*, 88. [[CrossRef](#)]
50. Bolyen, E.; Rideout, J.R.; Dillon, M.R.; Bokulich, N.A.; Abnet, C.C.; Al-Ghalith, G.A.; Alexander, H.; Alm, E.J.; Arumugam, M.; Asnicar, F.; et al. Reproducible, interactive, scalable and extensible microbiome data science using QIIME 2. *Nat. Biotechnol.* **2019**, *37*, 852–857. [[CrossRef](#)]
51. Edgar, R.C.; Haas, B.J.; Clemente, J.C.; Quince, C.; Knight, R. UCHIME improves sensitivity and speed of chimera detection. *Bioinformatics* **2011**, *27*, 2194–2200. [[CrossRef](#)]
52. Abarenkov, K.; Zirk, A.; Piirmann, T.; Põhönen, R.; Ivanov, F.; Nilsson, R.H.; Kõljalg, U. UNITE QIIME Release for Fungi. Version 8.2. 4 February 2020. UNITE Community. Available online: <https://plutof.ut.ee/#/doi/10.15156/BIO/786385> (accessed on 3 January 2022).
53. Bengtsson-Palme, J.; Ryberg, M.; Hartmann, M.; Branco, S.; Wang, Z.; Godhe, A.; De Wit, P.; Sánchez-García, M.; Ebersberger, I.; de Sousa, F.; et al. Improved software detection and extraction of ITS1 and ITS2 from ribosomal ITS sequences of fungi and other eukaryotes for analysis of environmental sequencing data. *Methods Ecol. Evol.* **2013**, *4*, 914–919. [[CrossRef](#)]
54. Heberle, H.; Meirelles, G.V.; da Silva, F.R.; Telles, G.P.; Minghim, R. InteractiVenn: A web-based tool for the analysis of sets through Venn diagrams. *BMC Bioinform.* **2015**, *16*, 169. [[CrossRef](#)] [[PubMed](#)]
55. Metsalu, T.; Vilo, J. Clustvis: A web tool for visualizing clustering of multivariate data using Principal Component Analysis and heatmap. *Nucleic Acids Res.* **2015**, *43*, W566–W570. [[CrossRef](#)] [[PubMed](#)]

56. White, T.; Bruns, T.; Lee, S.; Taylor, J. Amplification and direct sequencing of fungal ribosomal RNA genes for phylogenetics. In *PCR Protocols: A Guide to Methods and Applications*; Gelfand, D., Shinsky, J., White, T., Eds.; Academic Press, Inc.: New York, NY, USA, 1990; pp. 315–322.
57. Gardes, M.; Bruns, T.D. ITS primers with enhanced specificity for basidiomycetes application to the identification of mycorrhizae and rusts. *Mol. Ecol.* **1993**, *2*, 113–118. [[CrossRef](#)]
58. Altschul, S.F.; Madden, T.L.; Schäffer, A.A.; Zhang, J.; Zhang, Z.; Miller, W.; Lipman, D.J. Gapped BLAST and PSI-BLAST: A new generation of protein database search programs. *Nucleic Acids Res.* **1997**, *25*, 3389–3402. [[CrossRef](#)]
59. Crous, P.W.; Gams, W.; Stalpers, J.A.; Robert, V.; Stegehuis, G. MycoBank: An online initiative to launch mycology into the 21st century. *Stud. Mycol.* **2004**, *50*, 19–22.
60. Robert, V.; Stegehuis, G.; Stalpers, J. The MycoBank Engine and Related Databases. 2005. Available online: <https://www.MycoBank.org/> (accessed on 7 June 2022).
61. Shannon, P.; Markiel, A.; Ozier, O.; Baliga, N.S.; Wang, J.T.; Ramage, D.; Amin, N.; Schwikowski, B.; Ideker, T. Cytoscape: A Software Environment for Integrated Models of Biomolecular Interaction Networks. *Genome Res.* **2003**, *13*, 2498–2504. [[CrossRef](#)]
62. Trovão, J.; Portugal, A. Current Knowledge on the Fungal Degradation Abilities Profiled through Biodeteriorative Plate Essays. *Appl. Sci.* **2021**, *11*, 4196. [[CrossRef](#)]
63. Trovão, J.; Tiago, I.; Soares, F.; Paiva, D.S.; Mesquita, N.; Coelho, C.; Catarino, L.; Gil, F.; Portugal, A. Description of *Aeminiaceae* fam. nov., *Aeminium* gen. nov. and *Aeminium ludgeri* sp. nov. (Capnodiales), isolated from a biodeteriorated art-piece in the Old Cathedral of Coimbra. *MycKeys* **2019**, *45*, 57–73. [[CrossRef](#)]
64. Trovão, J.; Soares, F.; Paiva, D.S.; Tiago, I.; Portugal, A. *Circumfuscellium cavernae* gen. et sp. nov. (Bionectriaceae, Hypocreales) Isolated from a Hypogean Roman Cryptoporticus. *J. Fungi* **2022**, *8*, 837. [[CrossRef](#)]
65. Gautam, A.K.; Verma, R.K.; Avasthi, S.; Sushma; Bohra, Y.; Devadatha, B.; Niranjan, M.; Suwannarach, N. Current Insight into Traditional and Modern Methods in Fungal Diversity Estimates. *J. Fungi* **2022**, *8*, 226. [[CrossRef](#)]
66. Borrego, S.; Perdomo, I. Aerobiological investigations inside repositories of the national archive of the Republic of Cuba. *Aerobiologia* **2012**, *28*, 303–316. [[CrossRef](#)]
67. Borrego, S.; Perdomo, I. Airborne microorganisms cultivable on naturally ventilated document repositories of the National Archive of Cuba. *Environ. Sci. Pollut. Res.* **2016**, *23*, 3747–3757. [[CrossRef](#)]
68. Pyzik, A.; Ciuchcinski, K.; Dziurzynski, M.; Dziewit, L. The Bad and the Good—Microorganisms in Cultural Heritage Environments—An Update on Biodeterioration and Biotreatment Approaches. *Materials* **2021**, *14*, 177. [[CrossRef](#)]
69. Dziurzynski, M.; Ciuchcinski, K.; Dydka, M.; Szych, A.; Drabik, P.; Laudy, A.; Dziewit, L. Assessment of bacterial contamination of air at the museum of King John III's palace at Wilanow (Warsaw, Poland): Selection of an optimal growth medium for analyzing airborne bacteria diversity. *Appl. Sci.* **2020**, *10*, 7128. [[CrossRef](#)]
70. Pangallo, D.; Bučková, M.; Kraková, L.; Puškárová, A.; Šaková, N.; Grivalský, T.; Chovanová, K.; Zemánková, M. Biodeterioration of epoxy resin: A microbial survey through culture independent and culture-dependent approaches. *Environ. Microbiol.* **2015**, *17*, 462–479. [[CrossRef](#)]
71. Chaudhary, D.K.; Khulan, A.; Kim, J. Development of a novel cultivation technique for uncultured soil bacteria. *Sci. Rep.* **2019**, *9*, 1–11. [[CrossRef](#)] [[PubMed](#)]
72. Johann, L.; Alexandre, F.; Faisl, B. *Parengyodontium album*, a frequently reported fungal species in the cultural heritage environment. *Fungal Biol. Rev.* **2020**, *34*, 126–135. [[CrossRef](#)]
73. Horner, W.E.; Worthan, A.G.; Morey, P.R. Air- and dustborne mycoflora in houses free of water damage and fungal growth. *Appl. Environ. Microbiol.* **2004**, *70*, 6394–6400. [[CrossRef](#)]
74. Bensch, K.; Groenewald, J.Z.; Meijer, M.; Dijksterhuis, J.; Jurjević, Ž.; Andersen, B.; Houbraeken, J.; Crous, P.W.; Samson, R.A. Cladosporium species in indoor environments. *Stud. Mycol.* **2018**, *89*, 177–301. [[CrossRef](#)]
75. Zalar, P.; Hoog, G.S.; Schroers, H.J.; Crous, P.W.; Groenewald, J.Z.; Gunde-Cimerman, N. Phylogeny and ecology of the ubiquitous saprobe *Cladosporium sphaerospermum*, with descriptions of seven new species from hypersaline environments. *Stud. Mycol.* **2007**, *58*, 157–183. [[CrossRef](#)]
76. Jaouani, A.; Neifar, M.; Prigione, V.; Ayari, A.; Sbissi, I.; Ben Amor, S.; Ben Tekaya, S.; Varese, G.C.; Cherif, A.; Gtari, M. Diversity and enzymatic profiling of halotolerant micromycetes from sebkha el melah, a saharan salt flat in southern Tunisia. *BioMed Res. Int.* **2014**, *2014*, 439197. [[CrossRef](#)]
77. Basu, S.; Bose, C.; Ojha, N.; Das, N.; Das, J.; Pal, M.; Khurana, S. Evolution of bacterial and fungal growth media. *Bioinformation* **2015**, *11*, 182–184. [[CrossRef](#)]
78. Miller, A.Z.; Leal, N.; Laiz, L.; Candelera, R.; Silva, M.A.; Dionisio, A.; Macedo, M.F.; Sáiz-Jiménez, C. Primary bioreceptivity of limestones used in southern European monuments. *Geol. Soc. Lond. Spec. Publ.* **2010**, *331*, 79–92. [[CrossRef](#)]
79. Savković, Ž.; Stupar, M.; Unković, N.; Knežević, A.; Vukojević, J.; Grbić, M.L. Fungal Deterioration of Cultural Heritage Objects. In *Biodegradation Technology of Organic and Inorganic Pollutants*; Mendes, K.F., de Sousa, R.O., Mielke, K.C., Eds.; IntechOpen: London, UK, 2021. [[CrossRef](#)]
80. Li, Q.; Zhang, B.; He, Z.; Yang, X. Distribution and diversity of bacteria and fungi colonization in stone monuments analyzed by high-throughput sequencing. *PLoS ONE* **2016**, *11*, e0163287. [[CrossRef](#)] [[PubMed](#)]

81. Nowicka-Krawczyk, P.; Zelazna-Wieczorek, J.; Otlewska, A.; Koziróg, A.; Rajkowska, K.; Piotrowska, M.; Gutarowska, B.; Żydzik-Białek, A. Diversity of an aerial phototrophic coating of historic buildings in the former Auschwitz II-Birkenau concentration camp. *Sci. Total Environ.* **2014**, *493*, 116–123. [[CrossRef](#)]
82. Borderie, F.; Denis, M.; Barani, A.; Alaoui-Sossé, B.; Aleya, L. Microbial composition and ecological features of phototrophic biofilms proliferating in the Moidons Caves (France): Investigation at the single-cell level. *Environ. Sci. Pollut. Res.* **2016**, *23*, 12039–12049. [[CrossRef](#)] [[PubMed](#)]
83. Albertano, P.; Urzi, C. Structural interactions among epilithic cyanobacteria and heterotrophic microorganisms in Roman hypogea. *Microb. Ecol.* **1999**, *38*, 244–252. [[CrossRef](#)] [[PubMed](#)]
84. Ortega-Morales, B.O.; Narvaez-Zapata, J.A.; Schmalenberger, A.; Dousa-Lopez, A.; Tebbe, C.C. Biofilms fouling ancient limestone Mayan monuments in Uxmal, Mexico: A cultivation-independent analysis. *Biofilms* **2004**, *1*, 79–90. [[CrossRef](#)]
85. Roeselers, G.; van Loosdrecht, M.C.M.; Muyzer, G. Heterotrophic pioneers facilitate phototrophic biofilm development. *Microb. Ecol.* **2007**, *54*, 578–585. [[CrossRef](#)]
86. Sterflinger, K. Patination of marble at “Euromarble” exposure sites—iron stain versus bio pigments. In *Proceedings of the 9th Euromarble Eurocare EU 496*; Snethlage, R., Ed.; Workshop: Munich, Germany, 1999; pp. 83–91.
87. Urzi, C.; De Leo, F.; Salamone, P.; Criseo, G. Airborne fungal spores colonizing marbles exposed in the terrace of Messina Museum, Sicily. *Aerobiologia* **2001**, *17*, 11–17. [[CrossRef](#)]
88. Liua, B.; Fua, R.; Wu, B.; Liu, X.; Xiang, M. Rock-inhabiting fungi: Terminology, diversity, evolution and adaptation mechanisms. *Mycology* **2022**, *13*, 1–31. [[CrossRef](#)]
89. Isola, D.; Bartoli, F.; Meloni, P.; Caneva, G.; Zucconi, L. Black Fungi and Stone Heritage Conservation: Ecological and Metabolic Assays for Evaluating Colonization Potential and Responses to Traditional Biocides. *Appl. Sci.* **2022**, *12*, 2038. [[CrossRef](#)]
90. Benavente, D.; Sanchez-Moral, S.; Fernandez-Cortes, A.; Cañaveras, J.C.; Elez, J.; Saiz-Jimenez, C. Salt damage and microclimate in the Postumius Tomb, Roman Necropolis of Carmona, Spain. *Environ. Earth Sci.* **2011**, *63*, 1529–1543. [[CrossRef](#)]
91. Otlewska, A.; Adamiak, J.; Stryzewska, T.; Kańka, S.; Gutarowska, B. Factors Determining the Biodiversity of Halophilic Microorganisms on Historic Masonry Buildings. *Microbes Environ.* **2017**, *32*, 164–173. [[CrossRef](#)]
92. Piñar, G.; Ettenauer, J.; Sterflinger, K. La vie en rose: A review of rosy discoloration of subsurface monuments. In *The Conservation of Subterranean Cultural Heritage*; Saiz-Jimenez, C., Ed.; Taylor and Francis Group: London, UK, 2014; pp. 113–123.
93. Ruibal, C.; Platas, G.; Bills, G.F. Isolation and characterization of melanized fungi from limestone formations in Mallorca. *Mycol. Prog.* **2005**, *4*, 23–38. [[CrossRef](#)]
94. Ruibal, C.; Platas, G.; Bills, G.F. High diversity and morphological convergence among melanized fungi from rock formations in the Central Mountain System of Spain. *Persoonia* **2008**, *21*, 93–110. [[CrossRef](#)] [[PubMed](#)]
95. Selbmann, L.; de Hoog, G.S.; Mazzaglia, A.; Friedmann, E.I.; Onofri, S. Fungi at the edge of life: Cryptoendolithic black fungi from Antarctic desert. *Stud. Mycol.* **2005**, *51*, 1–32.
96. Selbmann, L.; de Hoog, G.S.; Zucconi, L.; Isola, D.; Ruisi, S.; Gerrits van den Ende, A.H.G.; Ruibal, C.; De Leo, F.; Urzi, C.; Onofri, S. Drought meets acid: Three new genera in a dothidealean clade of extremotolerant fungi. *Stud. Mycol.* **2008**, *61*, 1–20. [[CrossRef](#)] [[PubMed](#)]
97. Gorbushina, A.A.; Panina, L.K.; Vlasov, D.Y.; Krumbein, W.E. Fungi deteriorating Chersonesus marble. *Mikol. I Fitopatol.* **1996**, *30*, 23–28.
98. Sterflinger, K.; De Baere, R.; de Hoog, G.; De Wachter, R.; Krumbein, W.E.; Haase, G. *Coniosporium perforans* and *C. apollinis*, two new rock-inhabiting fungi isolated from marble in the Sanctuary of Delos (Cyclades, Greece). *Antonie Van Leeuwenhoek* **1997**, *72*, 349–363. [[CrossRef](#)] [[PubMed](#)]
99. Volkmann, M.; Gorbushina, A.A. A broadly applicable method for extraction and characterisation of mycosporines and mycosporine-like amino acids of terrestrial, marine and freshwater origin. *FEMS Microbiol. Lett.* **2006**, *255*, 286–295. [[CrossRef](#)]
100. Goordial, J.; Davila, A.; Lacelle, D.; Pollard, W.; Marinova, M.M.; Greer, C.W.; DiRuggiero, J.; McKay, C.P.; Whyte, L.G. Nearing the cold-arid limits of microbial life in permafrost of an upper dry valley, Antarctica. *ISME J.* **2016**, *10*, 1613–1624. [[CrossRef](#)]
101. Ruibal, C.; Gueidan, C.; Selbmann, L.; Gorbushina, A.A.; Crous, P.W.; Groenewald, J.Z.; Muggia, L.; Grube, M.; Isola, D.; Schoch, C.L.; et al. Phylogeny of rock-inhabiting fungi related to Dothideomycetes. *Stud. Mycol.* **2009**, *64*, 123–133. [[CrossRef](#)]
102. Alonso, L.; Creuzé-des-Châtelliers, C.; Trabac, T.; Dubost, A.; Moëgne-Loccoz, Y.; Pommier, T. Rock substrate rather than black stain alterations drives microbial community structure in the passage of Lascaux Cave. *Microbiome* **2018**, *6*, 216. [[CrossRef](#)]
103. Visagie, C.M.; Hirooka, Y.; Tanney, J.B.; Whitfield, E.; Mwange, K.; Meijer, M.; Amend, A.S.; Seifert, K.A.; Samson, R.A. *Aspergillus*, *Penicillium* and *Talaromyces* isolated from house dust samples collected around the world. *Stud. Mycol.* **2014**, *78*, 63–139. [[CrossRef](#)]
104. Chen, A.J.; Hubka, V.; Frisvad, J.C.; Visagie, C.M.; Houbraeken, J.; Meijer, M.; Varga, J.; Demirel, R.; Jurjević, Ž.; Kubátová, A.; et al. Polyphasic taxonomy of *Aspergillus* section *Aspergillus* (formerly *Eurotium*), and its occurrence in indoor environments and food. *Stud. Mycol.* **2017**, *88*, 37–135. [[CrossRef](#)] [[PubMed](#)]
105. Mesquita, N.; Soares, F.; Paiva de Carvalho, H.; Trovão, J.; Pinheiro, A.; Tiago, I.; Portugal, A. 6-Air and wall mycobiota interactions—A case study in the Old Cathedral of Coimbra. In *Viruses, Bacteria and Fungi in the Built Environment—Designing Healthy Indoor Environments*; Pacheco-Torgal, F., Ivanov, V., Falkinham, J.O., Eds.; Woodhead Publishing: Sawston, UK, 2022; Volume 1, pp. 101–125. ISBN 9780323852067.
106. Réblová, M.; Untereiner, W.A.; Réblová, K. Novel evolutionary lineages revealed in the chaetothyriales (fungi) based on multigene phylogenetic analyses and comparison of ITS secondary structure. *PLoS ONE* **2013**, *8*, e63547. [[CrossRef](#)] [[PubMed](#)]

107. Quaedvlieg, W.; Binder, M.; Groenewald, J.Z.; Summerell, B.A.; Carnegie, A.J.; Burgess, T.I.; Crous, P.W. Introducing the consolidated species concept to resolve species in the teratosphaeriaceae. *Persoonia* **2014**, *33*, 1–40. [[CrossRef](#)] [[PubMed](#)]
108. Isola, D.; Zucconi, L.; Onofri, S.; Caneva, G.; de Hoog, G.S.; Selbmann, L. Extremotolerant rock inhabiting black fungi from Italian monumental sites. *Fungal Divers.* **2016**, *76*, 75–96. [[CrossRef](#)]
109. Lee, S.H.; Park, H.S.; Nguyen, T.T.T.; Lee, H.B. Characterization of Three Species of Sordariomycetes Isolated from Freshwater and Soil Samples in Korea. *Mycobiology* **2019**, *47*, 20–30. [[CrossRef](#)]
110. Chiriví-Salomón, J.; Danies, G.; Restrepo, S.; Sanjuan, T. *Lecanicillium sabanense* sp. nov. (Cordycipitaceae) a new fungal entomopathogen of coccids. *Phytotaxa* **2015**, *234*, 063–074. [[CrossRef](#)]
111. Trovão, J.; Mesquita, N.; Paiva, D.S.; Paiva de Carvalho, H.; Avelar, L.; Portugal, A. Can arthropods act as vectors of fungal dispersion in heritage collections? A case study on the archive of the University of Coimbra, Portugal. *Int. Biodeterior. Biodegrad.* **2013**, *79*, 49–55. [[CrossRef](#)]
112. Ghobad-Nejhad, M.; Langer, E.; Nakasone, K.; Diederich, P.; Nilsson, R.H.; Rajchenberg, M.; Ginns, J. Digging Up the Roots: Taxonomic and Phylogenetic Disentanglements in Corticiaceae s.s. (Corticiales, Basidiomycota) and Evolution of Nutritional Modes. *Front. Microbiol.* **2021**, *25*, 2320. [[CrossRef](#)]
113. Qu, M.-H.; Wang, D.-Q.; Zhao, C.-L. A Phylogenetic and Taxonomic Study on *Xylodon* (Hymenochaetales): Focusing on Three New *Xylodon* Species from Southern China. *J. Fungi* **2022**, *8*, 35. [[CrossRef](#)]
114. Hussain, S.; Usman, M.; Afshan, N.-S.; Ahmad, H.; Khan, J.; Khalid, A.N. The genus *Coprinellus* (Basidiomycota; Agaricales) in Pakistan with the description of four new species. *MycKeys* **2018**, *39*, 111–126. [[CrossRef](#)]
115. Gordana, M.B.; Mikov, M.M.; Goločorbin-Kohn, S.M. The importance of genus *Candida* in human samples. *Zb. Matice Srp. Za Prir. Nauk.* **2008**, *114*, 79–95. [[CrossRef](#)]
116. Theelen, B.; Cafarchia, C.; Gaitanis, G.; Bassukas, I.D.; Boekhout, T.; Dawson, T.L., Jr. *Malassezia* ecology, pathophysiology, and treatment. *Med. Mycol.* **2019**, *57*, e2. [[CrossRef](#)] [[PubMed](#)]
117. Monteiro, G.A.; Vale, M.M.M. Occurrence of Yeast Species in Soils under Native and Modified Vegetation in an Iron Mining Area. *Rev. Bras. De Ciência Do Solo* **2018**, *42*, e0170375. [[CrossRef](#)]
118. Crous, P.W.; Carnegie, A.J.; Wingfield, M.J.; Sharma, R.; Mughini, G.; Noordeloos, M.E.; Santini, A.; Shouche, Y.S.; Bezerra, J.D.P.; Dima, B.; et al. Fungal Planet description sheets: 868–950. *Pers. Mol. Phylogeny Evol. Fungi* **2019**, *42*, 291–473. [[CrossRef](#)]
119. Burrow, K.; Grawunder, A.; Harpke, M.; Pietschmann, S.; Ehrhardt, R.; Wagner, L.; Voigt, K.; Merten, D.; Büchel, G.; Kothe, E. Microbiomes in an acidic rock-water cave system. *FEMS Microbiol. Lett.* **2019**, *366*, fnz167. [[CrossRef](#)]
120. Selbmann, L.; Stoppiello, G.A.; Onofri, S.; Stajich, J.E.; Coleine, C. Culture-Dependent and Amplicon Sequencing Approaches Reveal Diversity and Distribution of Black Fungi in Antarctic Cryptoendolithic Communities. *J. Fungi* **2021**, *7*, 213. [[CrossRef](#)]
121. Chen, J.; Gu, J.D. The environmental factors used in correlation analysis with microbial community of environmental and cultural heritage samples. *Int. Biodeterior. Biodegrad.* **2022**, *173*, 105460. [[CrossRef](#)]
122. Gonçalves, R.C.R.; Lisboa, H.C.F.; Pombeiro-Sponchiado, S.R. Characterization of melanin pigment produced by *Aspergillus nidulans*. *World J. Microbiol. Biotechnol. Vol.* **2012**, *28*, 1467–1474. [[CrossRef](#)]
123. Scrano, L.; Boccone, L.F.; Bufo, S.A.; Carrieri, R.; Lahoz, E.; Crescenzi, A. Morphological and molecular characterization of fungal populations possibly involved in the biological alteration of stones in historical buildings. *Commun. Agric. Appl. Biol. Sci.* **2012**, *77*, 187–195.
124. Gadd, G.M.; Bahri-Esfahani, J.; Li, Q.; Rhee, Y.J.; Wei, Z.; Fomina, M.; Liang, X. Oxalate production by fungi: Significance in geomycology, biodeterioration and bioremediation. *Fungal Biol. Rev.* **2014**, *28*, 36–55. [[CrossRef](#)]
125. Boniek, D.; de Castro Mendes, I.; Paiva, C.A.O.; de Paula Lana, U.G.; Dos Santos, A.F.B.; de Resende Stoianoff, M.A. Ecology and identification of environmental fungi and metabolic processes involved in the biodeterioration of Brazilian soapstone historical monuments. *Lett. Appl. Microbiol.* **2017**, *65*, 431–438. [[CrossRef](#)] [[PubMed](#)]
126. Skipper, P.J.A.; Skipper, L.K. A survey of bacterial colonization of historic limestone buildings: Lincoln Cathedral and St. Peter at Gowts, United Kingdom. In *Rehab 2014—Proceedings of the International Conference on Preservation, Maintenance and Rehabilitation of Historic Buildings and Structures*; Amoêda, R., Lira, S., Pinheiro, C., Eds.; Green Lines Institute: Barcelos, Portugal, 2014; Chapter 6; pp. 1003–1012.